2016

The Effect of Vibrations on Cryogens Boil Off During Launch, Transfer and Transport

Erin Schlichenmaier
University of Central Florida

THE EFFECT OF VIBRATION ON CRYOGENS BOIL-OFF DURING LAUNCH, TRANSFER AND TRANSPORT

by

ERIN SCHLICHENMAIER
B.S. Mechanical Engineering, University of Central Florida, 2003

A thesis submitted in partial fulfillment of the requirements
for the degree of Master of Science in Mechanical Engineering
in the Department of Mechanical and Aerospace Engineering
in the College of Engineering and Computer Science
at the University of Central Florida
Orlando, Florida

Summer Term
2016

ABSTRACT

Boil-off of a cryogenic fluid which is caused by the temperature difference between the fluid and its environment is a phenomenon which has long been studied and is well understood. However, vibrational excitation of a cryogenic storage tank and the fluid inside it also play a role in the loss of cryogens. Mechanical energy applied to the system in the form of vibrational input is converted into thermal energy via viscous damping of the fluid. As a result, when a storage tank full of cryogenic fluids is vibrated, it boils off at an increased rate.

A series of experiments were performed in which a cryogenic storage Dewar filled with liquid nitrogen was subjected to vibrational input and the rate of boil-off was measured. Based on the results of the testing, it has been determined that the rate of boil-off of a cryogenic fluid increases by a factor of up to five times the resting boil off rate during the application of vibrational energy. The development of advanced cryogenic storage systems capable of reducing vibrational loading of the fluid could significantly decrease the loss of cryogens during procedures such as transporting and storing the fluid or launching a space vehicle.

ACKNOWLEDGMENTS

The author wishes to express sincere appreciation to Dr. Louis Chow and Dr. Wei Wu for all of their assistance in the preparation of this thesis. In addition, special thanks to Rudy Werlink and James Fesmire at the NASA Cryogenics Test Laboratory and Mark Hamilton and Dan Ciarlariello at the NASA Vibrations Test Laboratory for all their hard work setting up and performing the necessary testing. This project was supported by the National Aeronautics and Space Administration through the University of Central Florida's NASA-Florida Space Grant Consortium.

TABLE OF CONTENTS

LIST OF FIGURES vi

LIST OF TABLES viii

ACRONYMS ix

CHAPTER 1 INTRODUCTION 1

1.1. Introduction 1

1.2. Project History 2

1.3. Scope of Work 3

CHAPTER 2 BACKGROUND 4

2.1. Cryogenics Overview 4

2.2. Vibrations Overview 6

2.2.1. The Frequency Response Function 7

2.2.2. The Half-Power Bandwidth Method 7

2.2.3. Filtering Data 9

2.2.4. Displacement 10

2.3. Energy 11

2.3.1. Mechanical Energy Absorbed 12

2.3.2. Thermal Energy Lost 14

2.3.1. Mechanical Energy Input 15

CHAPTER 3 EXPERIMENTAL DESIGN 17

3.1. Test Equipment 17

3.2. Test Development 21

CHAPTER 4 RESULTS AND ANALYSIS 24

4.1. Test Results 24
4.1.1. Input Data 25
4.1.2. Response Data 29
4.1.3. Filtering the Data 32
4.1.4. Creating Frequency Response Functions 36
4.1.5. Flow Meter Data 45
4.2. Analysis 49
4.2.1. Calculating Mechanical Energy Absorbed 49
4.2.2. Calculating Thermal Energy Lost 57
4.2.3. Total Energy 60
CHAPTER 5 CONCLUSION 61
5.1. Conclusion 61
APPENDIX MATLAB PROGRAM 62
LIST OF REFERENCES 70

LIST OF FIGURES

Figure 1 – Half Power Bandwidth Method 9

Figure 2 – Spring-Mass-Damper Model 12

Figure 3 – Electrodynamic Shaker System 18

Figure 4 – Test Configuration Diagram 19

Figure 5 – Test Configuration Photo 20

Figure 6 – Lab Test: Baseline Test With 10L Water 21

Figure 7 – Input Data Recorded by Accelerometers 26

Figure 8 – Input Data Recorded by Accelerometers (continued) 27

Figure 9 – Response Data 30

Figure 10 – Response Data (continued) 31

Figure 11 – Filter Visualization 33

Figure 12 – Comparison of Raw and Filtered Response Data 34

Figure 13 - Comparison of Raw and Filtered Response Data (continued) 35

Figure 14 – Frequency Response Functions 37

Figure 15 - Frequency Response Functions (continued) 38

Figure 16 – FRF Comparison Between Filtered and Unfiltered 40

Figure 17 - FRF Comparison Between Filtered and Unfiltered (continued) 41

Figure 18 – Frequency Response Functions, Filtered 43

Figure 19 - Frequency Response Functions, Filtered (continued) 44

Figure 20 – Flow Meter Data Overlaid with Response Data 46

Figure 21 – Frequency Response Function for 10L LN2 (.5 g) Test 49

Figure 22 – Closeup of Major Modes for 10L LN_2 (.5 g) Test 50

Figure 23 – Summary of Total Mechanical Energy Absorbed by System (W_{tot}) 56

Figure 24 – Total Thermal Energy Lost (E_t) 58

LIST OF TABLES

Table 1 – Properties of Water and Liquid Nitrogen 5

Table 2 – Mass of Dewar, Empty and Filled 17

Table 3 –Accelerometer Specifications 19

Table 4 – Tests Performed 23

Table 5 – Input Equations (Sinusoidal Sweep Only) 28

Table 6 – Maximum Flow Rate 48

Table 7 – Major Modes for Random Tests 51

Table 8 – Major Modes for Sine Sweep Tests 52

Table 9 - Q-Factor and Energy – Empty 53

Table 10 - Q-Factor and Energy – 5 L Water 54

Table 11 - Q-Factor and Energy – 5 L LN_2 54

Table 12 - Q-Factor and Energy – 10 L Water 54

Table 13 - Q-Factor and Energy – 10 L LN_2 55

Table 14 –Thermal Energy Lost by Systems 57

Table 15 –Thermal Energy Lost by Systems 59

Table 15 –Energy Loss Rate (Sine Sweep Tests) 60

Table 16 – Energy Loss Rate (Random Tests) 60

ACRONYMS

a_{max}	=	Acceleration
X_o	=	Amplitude
ω	=	Angular Velocity
ρ	=	Density
d_{max}	=	Displacement
W	=	Energy (Mechanical)
E_t	=	Energy (Thermal)
FFT	=	Fast Fourier Transform
$\dot{V}$	=	Flow Rate
f	=	Frequency
FRF	=	Frequency Response Function
A_{max}	=	Half-Power Bandwidth Amplitude
ΔH_{vap}	=	Heat of Vaporization
LN_2	=	Liquid Nitrogen
m	=	Mass
Q	=	Quality Factor (Q-Factor)
f_r	=	Resonant (Natural) Frequency
t	=	Time

CHAPTER 1

INTRODUCTION

1.1. Introduction

Cryogenic fluids such as liquid nitrogen, liquid oxygen and liquid hydrogen are used extensively by NASA and by private spaceflight companies in the continued support of the International Space Station and are critical to the future of space exploration. Cryogenic fluids are used for numerous space-related applications including refrigeration, life support, thermal control systems, scientific experiments, and liquid fuel propellants. Because cryogenic fluids are easily lost through heat leakage and boil-off of the fluid, the capability to efficiently store, transfer, and transport cryogens with minimal losses is essential.

Loss of cryogenic fluids resulting from heat transfer is a phenomenon which has long been studied and is well understood. Due to the large difference in temperature between a cryogenic fluid and its surrounding environment, there is a constant flow of thermal energy from the high temperature environment to the low temperature cryogenic fluid, heating the fluid and ultimately causing it to evaporate, or boil-off. Evaporation of a cryogenic fluid occurs at the surface layer; impurities in the surface and mechanical disturbances of the surface can lead to instabilities in the rate of boil off or to vapor explosions [1]. The development of containers with high thermal insulative properties capable of storing cryogenic fluids have been investigated and developed since the 1880's when Sir James Dewar invented the earliest insulated storage systems [1]. Since then, the technology of cryogenics has been expanded greatly, and storage containers have been

developed which are highly effective at mitigating the loss of cryogenic fluids due to thermal differentials.

However, the application of vibrational energy to a cryogenic storage system can also have an effect on the rate of boil off of the supercooled liquid. Vibration of the storage container causes the cryogenic fluid within to vibrate and the viscosity of the fluid acts as a damper, absorbing some of the vibrational energy of the system. As the fluid absorbs energy its temperature increases, leading the rate of boil-off of the fluid to increase regardless of the associated thermal insulation of the container. Better understanding the conversion of energy from mechanical to thermal could lead to the development of advanced cryogenic systems which, in addition to providing thermal protection, would also be capable of mitigating the energy losses caused by vibration, decreasing the overall loss of cryogenic fluids.

1.2. Project History

During testing at the NASA Vibrations Test Laboratory and the NASA Cryogenics Test Laboratory at the Kennedy Space Center in 2012, a ten liter storage Dewar filled with liquid nitrogen was excited using a vibration table [2]. The test was intended to study the insulative properties of the cryogenic storage container itself, specifically the performance of the Aerogel bead insulation and MLI layered insulation and the effect of drop shock effects on the storage system [2]. During the experiment it was observed that the quantity of nitrogen vapors emanating from the Dewar increased significantly during the application of vibrational loading and then returned to a lower steady state rate when the system was at rest [2]. The increased rate of vapor emissions indicated that the rate of boil off of the liquid nitrogen had increased due to the application mechanical energy to the system in the form of vibration.

This observation raised the question as to exactly how the energy was transferred from mechanical energy input to thermal energy output and how that energy conversion could be expressed mathematically. It was decided to perform additional testing in order to explore this phenomenon further.

1.3. Scope of Work

In order to better understand the conversion of mechanical energy to thermal energy, several additional tests were performed at the Kennedy Space Center Vibrations Test Laboratory. The major goal of this project was to create a test set-up capable of vibrating a cryogenic storage Dewar full of liquid nitrogen while precisely measuring the rate of flow of nitrogen vapors exiting the system. The testing would need to be conducted in several stages: the first stage was to perform baseline vibrational testing on the test set-up; the second step was to perform baseline testing with the container full of water; and the final step was to perform vibrational testing with the container full of liquid nitrogen while using a flow meter to monitor the rate of boil off. By comparing the results of the baseline tests with the results of the liquid nitrogen testing, it would be possible to determine how much mechanical energy was being absorbed by the system, how much thermal energy was being released, and how those quantities changed during the application of vibrational loading to the storage system.

This project was supported by the National Aeronautics and Space Administration through the University of Central Florida's NASA-Florida Space Grant Consortium.

CHAPTER 2

BACKGROUND

2.1. Cryogenics Overview

Cryogenics is the branch of physics which focuses on the effects of very low temperatures on a variety of materials. More specifically, cryogenics deals with temperatures at or below 120 K (-243.7° F) because it is in this range that common atmospheric gases such as oxygen, nitrogen and hydrogen have been cooled below their boiling point and can exist in a liquid state at atmospheric pressure. These extremely cold cryogenic liquids are utilized in a wide range of applications including use in chemical and metallurgical processes, separation of gases, cooling for equipment such as lasers and medical instruments, fuel for hydrogen vehicles, refrigerants and coolants, and liquid propellants for rockets.

Liquid nitrogen is one of the most commonly used cryogenic fluids for numerous reasons. Liquid nitrogen is easy to produce and widely available. It can be stored at atmospheric pressure with no additional pressurization required to maintain its liquid state. Another benefit to the use of liquid nitrogen is that its physical properties are very similar to those of water, specifically in terms of density and viscosity [3]. This similarity means that water can be used to simulate the response of liquid nitrogen with a high level of accuracy. The physical properties of liquid nitrogen and water are listed in Table 1, as well as the properties of liquid helium, for comparison purposes [3].

Table 1 – Properties of Water and Liquid Nitrogen

	Water	LN2	Helium
Boiling Point at atmospheric pressure (K)	373	77	4.2
Dynamic viscosity of liquid [1] (μPl)	278	152	3.3
Liquid density [1] ($\frac{kg}{m^3}$)	960	808	125
Heat of vaporization [1] ($\frac{kJ}{kg}$)	2260	199	20.4

(1) at normal boiling point

In ideal steady-state conditions where the cryogenic liquid level in the storage container is maintained at a perfectly constant level, the vapor flow escaping the container would precisely equal the rate of boil-off of the fluid [3]. However in real world conditions, as boil off occurs the level of liquid in the container steadily drops and the volume of empty space in the container increases. A portion of the newly evaporated nitrogen remains inside the container in its gaseous state to fill the increased volume and as a result, the volume of gas actually escaping the container no longer perfectly represents the true reduction in volume of the liquid that has occurred. This is true for any cryogenic fluid and can be accounted for using a simple correction factor. For a material such as hydrogen, the correction factor is 1.16 and the effect must be taken into account when measuring the amount of vapor escaping the container with a flow meter [3]. For liquid nitrogen however, the correction factor is only 1.006; in this case the effect can be considered to be negligible and can be ignored [3]. This is another reason why liquid nitrogen is an ideal material to be used in any experiment in which the rate of boil off or the flow rate of the escaping vapor will be considered because the volume measurements recorded by the flow meter can be used directly without correction [3].

2.2. Vibrations Overview

A vibrating system is a mechanical system which undergoes oscillatory motion over time. This oscillatory motion can be repetitive, where the amplitude of the oscillations repeat at regular time intervals, or it can be random, where there is no apparent pattern to the amplitude of the vibrations. Once set into motion, an oscillating system will continue its vibration indefinitely unless a damping force acts to reduce the motion. For a mechanical system made up of rigid bodies in motion, damping forces most often consist of friction or some other externally applied force [4]. In a system which includes liquids, the viscosity of the liquid itself acts as an additional damping force.

For simple systems, the motion of the system can be fully described with just a few equations. However, real mechanical systems are rarely as simple as a single mass system such as a pendulum or a spring and mass. Vibrations associated with a real mechanical system undergoing oscillatory motion may be quite complicated and the equations used to describe such a system are not as obvious. However, the motion of a complex system can usually be reduced mathematically to a set of linear motions called normal modes which allows the motion of the system to be described as a collection of simple one-mass linear systems [4]. It is necessary to perform vibrational testing in order to find the normal modes for a particular system.

In order to discover its natural frequencies, a given system is subjected to a range of vibrations with accelerometers attached to various points of the test set up to record the response of the components. The system can be subjected to a sequential range of increasing or decreasing frequencies (a sinusoidal sweep), or it can be subjected to a wide range of frequencies all at once (random) [5]. The amplitude will reach one or more peaks where the amplitude spikes by an order

of magnitude. With enough accelerometers attached in strategic locations, a highly accurate mathematical model of the system can be created.

2.2.1. The Frequency Response Function

The tool most commonly used to analyze and understand data gathered during a vibration test is the frequency response function (FRF). The FRF characterizes the dynamics of a system through the relationship between the input and the output signals [6]. In order to calculate the frequency response function for a given system, the input and output data sets are first converted from the time domain to the frequency domain by applying a fast Fourier transform (FFT) to each data set [7]. For a linear system with a single input and a single output, the frequency response function is simply the ratio of the output signal in the frequency domain to the input signal in the frequency domain, as shown in Equation (1).

$$H(\omega) = \frac{\mathcal{F}(y(t))}{\mathcal{F}(x(t))} \tag{1}$$

Plotting the frequency response function in the frequency domain reveals important data about the test, specifically the location and magnitude associated with each of the resonant frequencies of the system.

2.2.2. The Half-Power Bandwidth Method

The quality factor, or Q-factor, is a measure of the damping of the system, or a measure of how quickly the motion of a vibrating system decays. The Q-factor is not measured in terms of

time; it is represented as the number of cycles required for the motion to decay to equilibrium and is proportional to the natural frequency of the system divided by the system damping [4]. The lower the damping, the longer it takes for the system to reach equilibrium, and the higher the Q-factor [4] [8]. On a frequency-response curve, a natural frequency with a very tall, sharp peak is indicative of a system with a high Q-factor and low damping; a natural frequency with a short, wide peak indicates a system with a low Q-factor and a high damping effect.

When the damping for a system is unknown, the Q-factor can be determined from the frequency-response curve utilizing the half power bandwidth method. First the natural frequencies (f_r) of each of the relevant modes are found. Then the half power bandwidth frequencies (f_a and f_b) are determined by dividing the amplitude of the natural frequency at a natural mode by $\sqrt{2}$ and drawing a horizontal line across the frequency-response curve at the resulting half power amplitude. The frequencies at which the horizontal line crosses the frequency-response curve are the half power bandwidths (f_a and f_b) [9]. The relationship between the amplitude associated with the resonant frequency and the half power bandwidth amplitudes is shown in Figure 1.

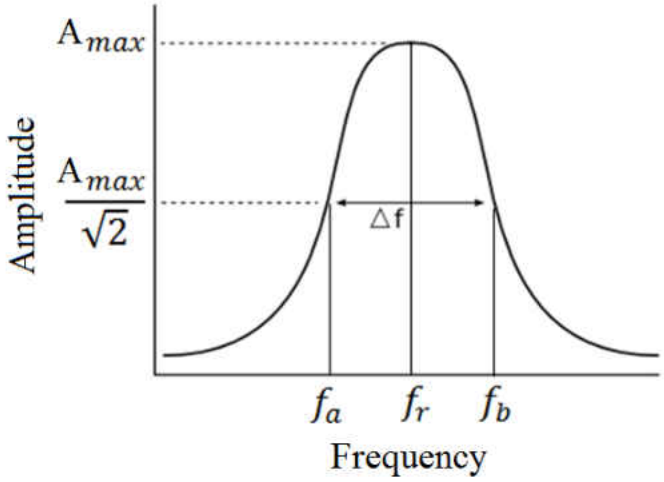

Figure 1 – Half Power Bandwidth Method

Once the natural frequency and the half-power bandwidth frequencies are known, the Q-factor can be calculated by dividing the value of the natural frequency (f_r) by the difference in the half power bandwidth frequencies (f_a and f_b) as shown in Equation (2).

$$Q = \frac{f_r}{\Delta f} = \frac{f_r}{f_b - f_a} \tag{2}$$

The Q-factor represents the damping for a system and once known, can then be used to calculate the energy of a vibrating system.

2.2.3. Filtering Data

It is often necessary to process or to filter the input and response data obtained during vibrational testing in order to remove noise, perform data averaging, and to clarify and highlight important patterns. Noise may be introduced to a set of results as electrical noise in the

measurement system, mechanical vibrations in the environment which are outside the scope of the test, or due to carrier frequency rectification effects.

A digital signal filter is essentially a circuit which has been designed to remove frequencies in certain ranges while allowing others to pass [5]. While there are some cases where both low and high frequencies may need to be filtered out of the data, the source of extraneous data is most often contained with the high frequency range [5]; in these cases, a low-pass filter is used to reduce the effect of this noise. Ideally, a filter would be capable of completely rejecting the unwanted frequencies and passing the desirable frequency range; however such a perfect filter does not exist [10]. Instead, a variety of filters have been created which offer various compromises in the way the data is processed. The most commonly used low pass filter is the Butterworth Filter, which offers a very good flat response in the pass band, a rapid drop to zero in the stop band, and no ripple effect in the stop band frequencies [5].

2.2.4. Displacement

In theory, the displacement of a system can be calculated by double integrating the acceleration data gathered by the accelerometers. However in practice, the double integration method often does not yield accurate displacement results due to over-amplification of the low frequency components of a given signal [11]. Recording the acceleration using digital accelerometers allows for small distortions which become amplified with each integration until the displacement data is no longer accurate [11]. A high pass filter can often be used to reduce the effect of the baseline offsets and produce usable displacement results, however in this case, attempts to utilize a high pass filter to clean up the acceleration data showed no measurable

improvement to the results of the double integration. Instead, the displacement will be calculated using Equation (3) [11].

$$d_{max} = \frac{a_{max}}{\omega_n^2} \tag{3}$$

A harmonic vibration with a known frequency of ω_n (in radians) and known acceleration a_{max} results in displacement of d_{max} [11]. The result of this calculation yields the displacement in meters.

It shall be noted that for the purposes of this experiment, it was possible to use this method to calculate the displacement for each of the major modes for each of the sinusoidal sweep tests. However, due to the method of analysis of the results, it was not possible to use the same method in order to calculate the displacement for the random tests. It was difficult to isolate the resonant frequencies in the response data in order to be able to determine the magnitude of the associated acceleration at any given point. As a result, it has been assumed that the displacement for each of the major modes of the random tests would be equivalent to the displacement for the major modes of the sinusoidal sweep test as long as the modes had sufficiently similar resonant frequencies and maximum accelerations.

2.3. Energy

Mechanical energy applied to the system in the form of vibrations is converted into thermal energy via viscous damping of the fluid. As a result, it is necessary to calculate the total

amount of mechanical energy absorbed by the system and the total amount of thermal energy lost by the system in order to determine the effect viscous damping of the fluid is having on energy loss.

2.3.1. Mechanical Energy Absorbed

The cryogenic storage Dewar used in the tests consists of an outer and an inner tank which are connected at the annulus, or the neck. For the purposes of the test, the outer tank can be considered to be rigid and is attached directly to the vibration table. The mass of the fluid is contained within the inner tank and the flexibility of the connection between the two shells of the tank allows for the inner tank to move somewhat independently of the outer tank. As a result, the cryogenic storage system can be approximately modeled as a Mass-Spring-Damper system as shown in Figure 2, where the mass hangs supported below a spring and a damper.

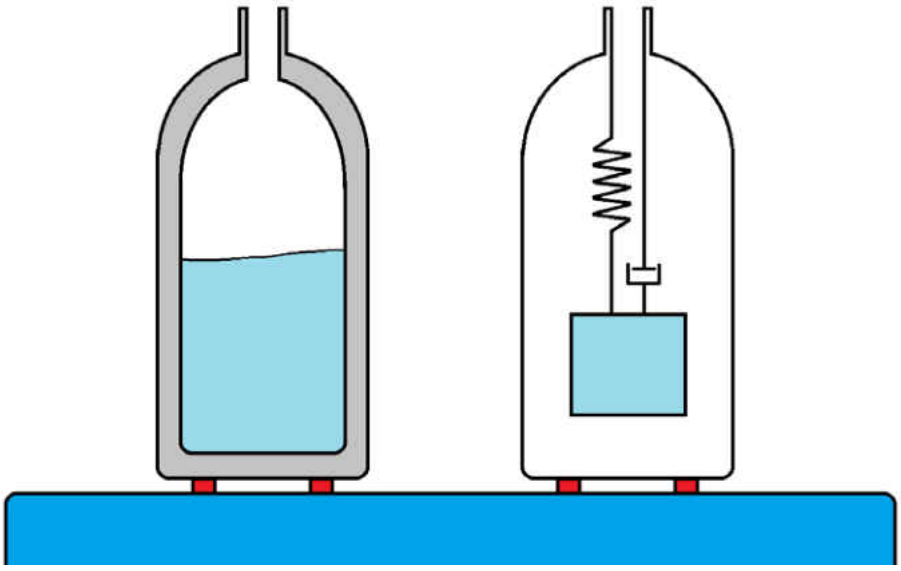

Figure 2 – Spring-Mass-Damper Model

The energy absorbed by a simple system with a single resonant frequency mode can be determined using Equation (4) [12].

$$W = \frac{mQ^{-1}\omega^3 {X_o}^2}{2} \tag{4}$$

For a system that experiences more than one natural mode as most real-world systems do, the total energy input to the system is the sum of the energy at all of the major modes of excitation frequency. Therefore, the total energy input to the system would be determined using the summation given in Equation (5).

$$W_{total} = \sum_{n=1}^{N} \frac{mQ_n^{-1}\omega_n^3 X_{on}^2}{2} \tag{5}$$

The term (m) is the mass of the system in kilograms and is determined simply by weighing the tank in its various configurations. The Q-factor for each major mode (Q_n) is calculated from the resonant frequency using the half-power bandwidth method described in the previous section. The (ω_n) variable is simply the resonant frequency in radians. And finally, (X_{on}) is the displacement in meters at the resonant frequency. The resulting energy (W_{tot}) is measured in watts.

Typically, only the first few modes are found to be significant and the energy associated with the remaining modes can be considered to be negligible. Performing vibrational testing on the Dewar will determine the major modes of the system. Once the major modes have been

determined, the damping factor can be determined for each major mode and the energy absorbed at each major mode can be calculated in turn using the previously described set of equations.

An important point to note is that the system is modeled as a spring-mass-damper system where the spring is located above the mass and where the mass is not a single solid unit but is a fluid. As a result, the most important information about the amplitude of motion is obtained at the bottommost point of the motion. This is where the mass has stretched the spring to its extreme and the liquid itself is compressed into the bottom of the container and can effectively be considered a single continuous mass. The topmost points of motion are where it is possible for the liquid not to be in a single contained mass, for example, the liquid may splash within the Dewar, and the exact amplitude at the upper point of motion may be imprecise.

2.3.2. Thermal Energy Lost

The thermal energy lost by the system is simple to determine. The flow meter at the sealed nozzle of the Dewar measures the rate of flow of the evaporated nitrogen exiting the system. Recall that for liquid nitrogen, the amount of vapor escaping the Dewar equals the rate of boil off of the material; losses due to the change in volume of the liquid inside the container can be considered negligible and no correction factor is required. The rate of flow of nitrogen gas exiting the system will be monitored before, during, and after each vibrational test. By measuring exactly how much vapor exited the system during each test, the amount of boil off will be known and the increased amount of thermal energy leaving the system is easily found.

The amount of thermal energy exiting the system at any given time is equal to the heat of vaporization (ΔH_{vap}) for the liquid multiplied by the density of the liquid (ρ) multiplied by the flow rate ($\dot{V}$), as shown in Equation (6).

$$E_t = \Delta H_{vap} \dot{V} \rho \tag{6}$$

The heat of vaporization and density are known physical properties associated with liquid nitrogen at a given temperature and pressure and the flow rate is measured using a flow meter during experimental testing.

2.3.1.Mechanical Energy Input

The amount of energy input into the system can be determined in two ways. One method is to use data gathered by accelerometers bonded to the shaker table top. This method is quite accurate but could potentially become time consuming and requires a computer to perform the necessary calculations on a very large number of data points.

The other method is the mapping method. In this method, an equation is used to represent the frequencies input into the system. For cases where an accurate equation can be found, this is the much simpler method because a single equation can be used in place of a very large amount of gathered test data. However, not all tests input profiles can be summarized into a single equation; for example, if the input is applied randomly, no simple equation could be written to represent the input frequencies. For a test where the input is a sinusoidal sweep through a

range of frequencies, an equation can easily be found. For this series of tests, the recorded test acceleration data will be used for the mechanical energy input.

CHAPTER 3

EXPERIMENTAL DESIGN

3.1. Test Equipment

The cryogenic storage container used for testing was a D200 ten liter, aluminum cryogenic storage Dewar. The container consists of two layers, an outer shell and inner vessel which are connected by a neck tube at the top. The container also has two evacuating nozzles near the neck to prevent pressure buildup between the inner and outer tanks. The mass of the empty tank and the masses of the various configurations are shown in Table 2.

Table 2 – Mass of Dewar, Empty and Filled

Configuration (LN_2)	Mass (kg)	Mass (lb)	Configuration (Water)	Mass (kg)	Mass (lb)
Empty Tank	5.9	13.0	Empty Tank	5.9	13.0
5 Liters of Water	5.0	11.0	5 Liters of LN_2	4.0	8.9
Tank Plus 5 Liters Water	10.9	24.0	Tank Plus 5 Liters LN_2	9.9	21.8
Tank Plus 10 Liters Water	15.9	35.0	Tank Plus 10 Liters LN_2	13.9	30.6

The volume between the inner and outer tanks, called the intertank annulus, was filled with Cabot grade P100 Aerogel Particles. Aerogel is a dry, porous, extremely low density material which consists of more than 95% air by volume [13] and the density is only 80 to 100 kg/m^3 [14]. The material that makes up the porous structure itself is made of 97% pure silica. The pores in the material are so small that gas phase heat conduction is very poor [13]. It is the low density of the

aerogel as well as the unique structure of the material which makes it such an effective thermal insulator.

Vibration testing was completed using an Unholtz-Dickie model 2XSAI240-T-1000-32LH/ST Electrodynamic Shaker System. The vibration table is designed to achieve a generated force continuous rating 22,000 pounds peak for sine tests and 20,000 pounds RMS for random tests, based on a flat spectrum with 1,000 pound payload. The table is capable of up to 200 g maximum free table acceleration and up to a one inch peak-to-peak shaker stroke in the vertical direction or z-direction [15]. The shaker system is shown in Figure 3.

Figure 3 – Electrodynamic Shaker System

Source: Kennedy Space Center Engineering Directorate, Materials Science Division, Vibration Testing Lab, Kennedy Space Center

A total of five accelerometers were mounted in various locations on the test set up and storage tank to gather test data. Three triaxial PCB accelerometers were mounted to the surface of the shaker table. One uniaxial Unholtz-Dickie accelerometer was mounted to the outside of the

tank near the neck and one uniaxial Unholtz-Dickie accelerometer was bonded to the inside bottom surface of the inner tank. The exact specifications for each of the accelerometers is listed in Table 3. A diagram for the configuration of the set up and the location of the accelerometers is shown in Figure 4.

Table 3 –Accelerometer Specifications

Location	Manufacturer	Nominal Sensitivity	Measurement Range	Frequency Range
Shaker Table Surface	PCB	10 mV/g	+/- 500 g pk	2 – 8,000 Hz
Outer Tank	Unholtz-Dickie	10 pC/g	+/- 1000 g pk	10 – 10,000 Hz
Inner Tank	Unholtz-Dickie	10 pC/g	+/- 1000 g pk	10 – 10,000 Hz

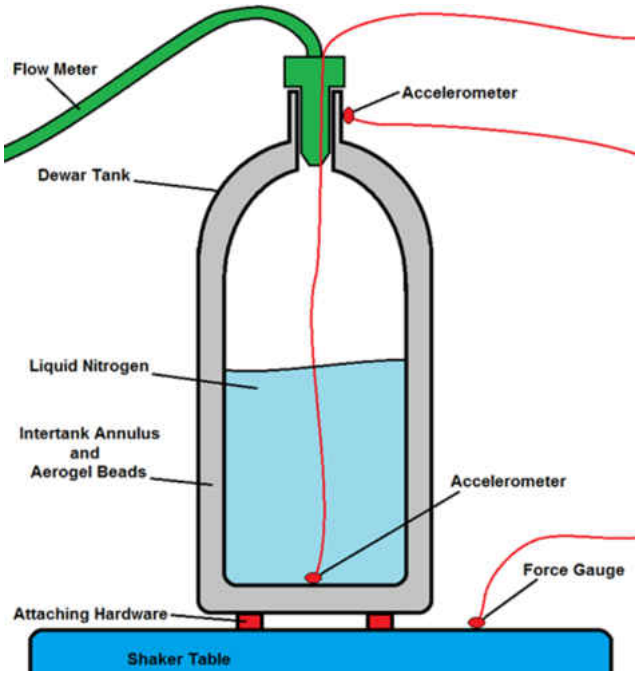

Figure 4 – Test Configuration Diagram

A photo of the full test set up, with the ten liter cryogenic storage Dewar mounted to the shaker table, the flow meter installed at the neck of the tank, and the accelerometers mounted in place, is shown in Figure 5.

Figure 5 – Test Configuration Photo

The flow meter used was an MKS 0-5 volt flow meter. For this model, 5 volts equals 20,000 standard cubic centimeters per minute; which means that each volt is equal to 4 liters per minute.

The remainder of the test setup included high speed cameras to record the testing. All testing was performed at the NASA Vibration Testing Laboratory and Cryogenic Testing

Laboratory located at the Kennedy Space Center. Figure 6 shows a view of the vibrations lab, the test set up, and two of the data monitors.

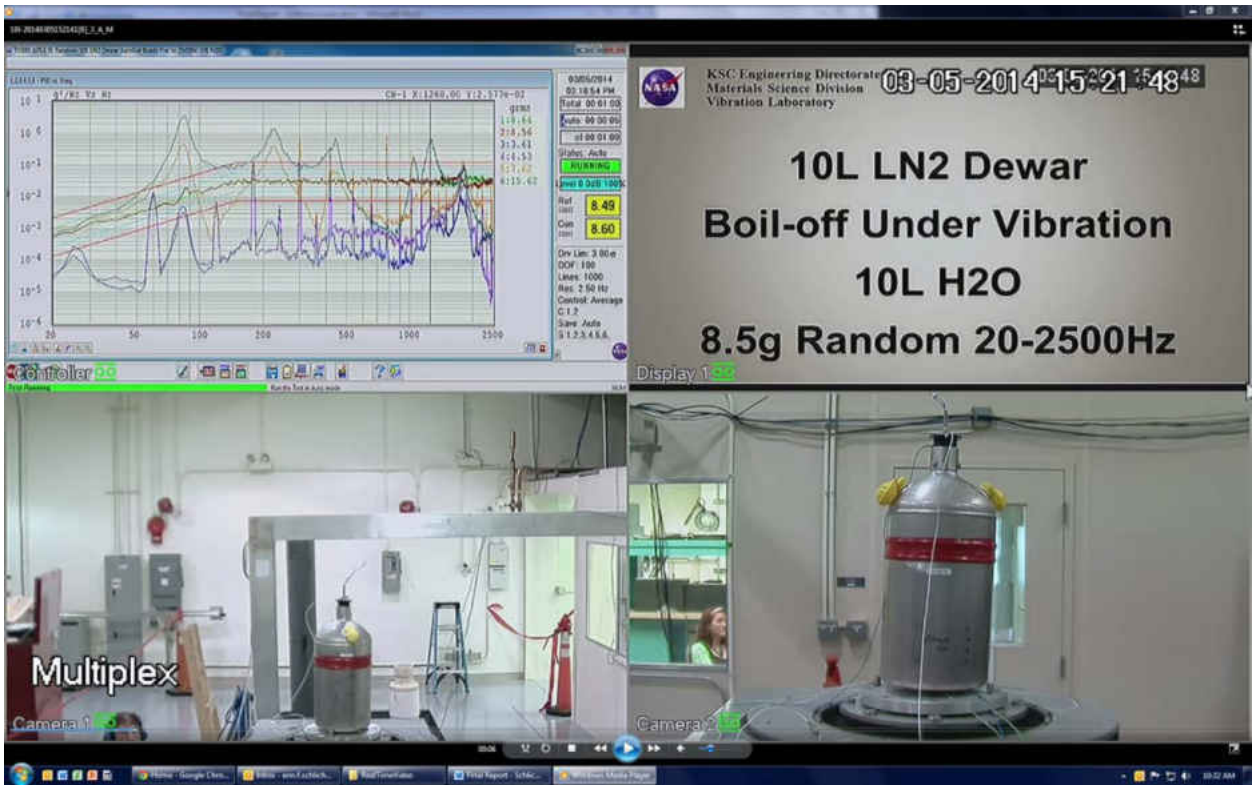

Figure 6 – Lab Test: Baseline Test With 10L Water

Source: Kennedy Space Center Engineering Directorate, Materials Science Division, Vibration Testing Lab, Kennedy Space Center

3.2. Test Development

The first phase of testing was required to verify the test configuration and to determine the baseline natural frequencies of the testing configuration. For the initial set up phase, three different configurations were tested: the empty Dewar, the Dewar filled with five liters of water, and the Dewar filled with ten liters of water. Because water and liquid nitrogen share similar

viscosities and densities, the damping effect of the water would make a suitable baseline to compare to the damping effect of the liquid nitrogen. Each configuration was subjected to a sinusoidal sweep test and a random test in the range of frequencies a cryogenic storage system would most likely be subjected to during a launch. The sine sweep test consisted of a steady sweep of the frequencies between 5Hz and 2,500Hz over the course of four to five minutes while the random sweep test consisted of random excitation in the range of 5Hz to 2,500Hz for approximately one minute. While random vibration testing is often more a more realistic representation of real-world conditions, the sinusoidal sweep testing often leads to cleaner modal responses and can result in data that is more useful for evaluation [16].

The second stage of the testing was to determine the nominal, steady-state rate of boil off of the liquid nitrogen with the system at rest. The tank was filled with ten liters of liquid nitrogen and fitted with the flow meter sealing the neck of the tank. The rate of flow was monitored as the LN_2 was allowed to boil-off with the entire system at rest in order to determine the resting boil off rate.

Once the baseline information was gathered about the test configuration, then the third and final phase of testing was performed. In this stage, the tank was capped with the flow meter and the system was subjected to the same set of sine sweep and the random vibration tests as were performed in the set up tests, this time with first five liters and then with ten liters of liquid nitrogen. A list of all of the tests performed and the parameters associated with each test is given in Table 4.

Table 4 – Tests Performed

Test	Test Type	Frequency Range (Hz)	Time (seconds)	Acceleration
Empty	Random	20-2500	80	8.5 grms
Empty	Sweep	5-2500	300	0.5 g
5 Liters Water	Random	20-2500	80	8.5 grms
5 Liters Water	Sweep	2500-5	300	0.5 g
5 Liters LN2	Random	20-2500	70	8.5 grms
5 Liters LN2	Sweep	5-2500	300	0.5 g
10 Liters Water	Random	20-2500	80	8.5 grms
10 Liters Water	Sweep	2500-5	300	0.5 g
10 Liters LN2	Random	20-2500	80	8.5 grms
10 Liters LN2	Sweep	2000-5	600	0.5 g
10 Liters LN2	Sweep	2000-20	600	1.0 g

CHAPTER 4

RESULTS AND ANALYSIS

4.1. Test Results

A total of eleven tests were performed during this experiment, including a sinusoidal sweep and a random frequency test for each of the five configurations: empty tank, tank filled with five liters of water, tank filled with ten liters of water, tank filled with five liters of liquid nitrogen, and tank filled with ten liters of liquid nitrogen. In order to gather additional data about the rate of boil off of the liquid nitrogen, two sine sweep tests were performed in the case of the tank filled with ten liters of liquid nitrogen, one sinusoidal sweep at an average input of one g and one sinusoidal sweep at an average input of one-half g.

Analyzing the test data consists of multiple steps. The first step is to compile and plot the collected input data and the response data. Then the collected data must be filtered to remove noise and unwanted data points. The filtered input and response data is then converted to the frequency domain using a fast Fourier transform and from this, the frequency response function is calculated and plotted in the frequency domain. Next, the major resonant frequencies and the amplitude at those frequencies can be determined, as well as the Q-factors for each major mode. Then the energy absorbed by the system can be calculated using the half-power bandwidth method. Once all of the information about energy input to the system and absorbed by the system has been gathered or calculated, the last step is to evaluate the flow meter data in order to compare the energies to determine the effect of vibrations on the rate of boil off of the cryogenic fluid.

4.1.1. Input Data

The input to the system was recorded by the accelerometers attached to the shaker table surface to record the vibrational energy input by the table itself. A summary of the raw input data gathered during each experiment is given in Figure 7 and Figure 8.

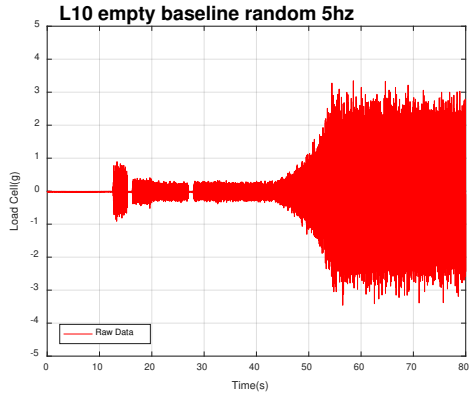

Empty Random

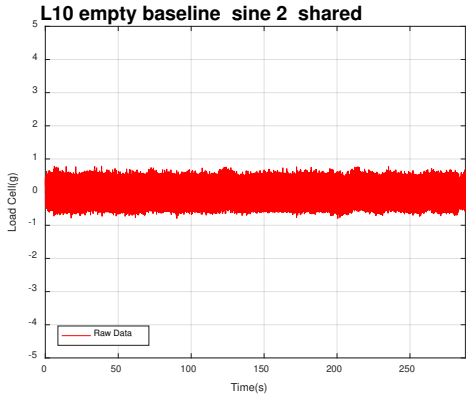

Empty Sine

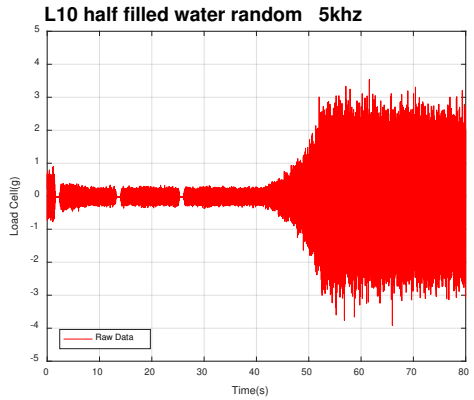

5L Water Random

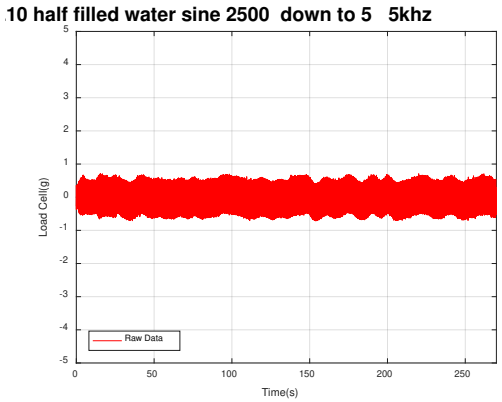

5L Water Sine

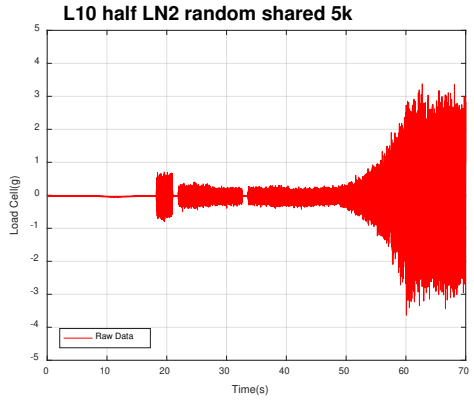

5L LN2 Random

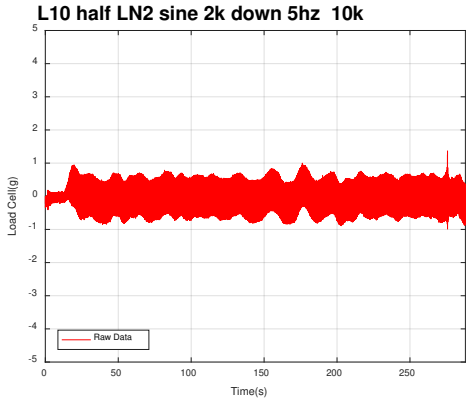

5L LN2 Sine

Figure 7 – Input Data Recorded by Accelerometers

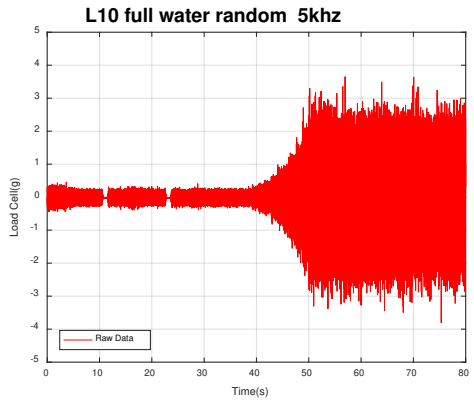

10L Water Random

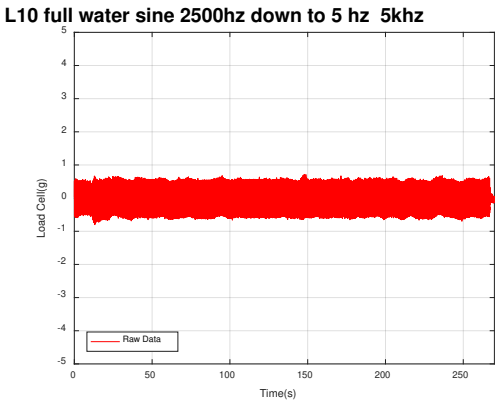

10L Water Sine

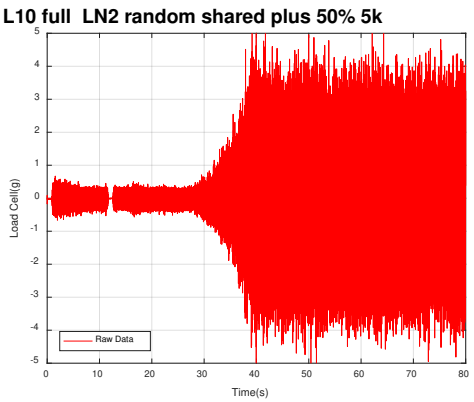

10L LN2 Random

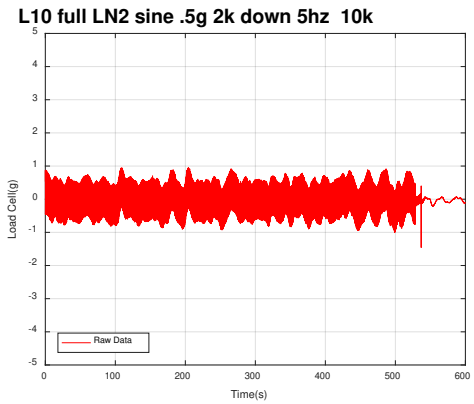

10L LN2 Sine (0.5 g)

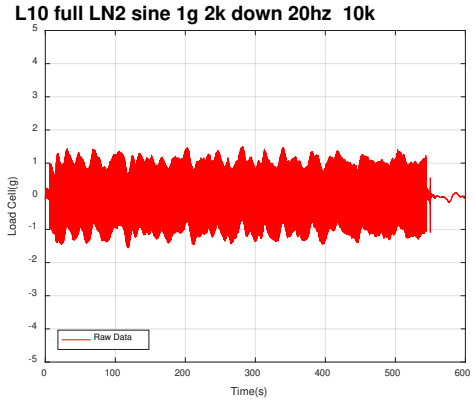

10L LN2 Sine (1 g)

Figure 8 – Input Data Recorded by Accelerometers (continued)

Note that for each of the tests which utilized random input, there is a period of time during which the amplitude of the acceleration of the shaker table is small before the table ramps up to full speed and amplitude. This data has been kept in order to preserve the timeline and the full response data associated with the test.

For each of the six sinusoidal sweep tests performed, an equation can be found which approximates the frequencies of the vibration applied to the system. Because the input frequencies for the random tests were applied randomly, no equation can be written to represent the input frequencies. A summary of the input energy equations for each of the sinusoidal sweep tests is given in Table 5.

Table 5 – Input Equations (Sinusoidal Sweep Only)

Test	Input Frequency Equation
Empty	$F = 5e^{0.0207t}$
5 Liters Water	$F = 2500e^{-0.0207t}$
5 Liters LN2	$F = 5e^{0.0207t}$
10 Liters Water	$F = 2500e^{-0.0207t}$
10 Liters LN2 (0.5 g)	$F = 2000e^{-0.0099t}$
10 Liters LN2 (1 g)	$F = 2000e^{-0.0076t}$

These equations could be used to calculate the energy input into the system for the sine sweep tests, however, since the input energy was measured by the accelerometers for both the sine and the random tests, the recorded data will be used to represent the input in order to be as accurate as possible and in order to be consistent between the tests.

4.1.2. Response Data

The response data was gathered from the accelerometer mounted to the inner bottom surface of the inner tank. A summary of the response data gathered during each experiment is give in Figure 9 and Figure 10.

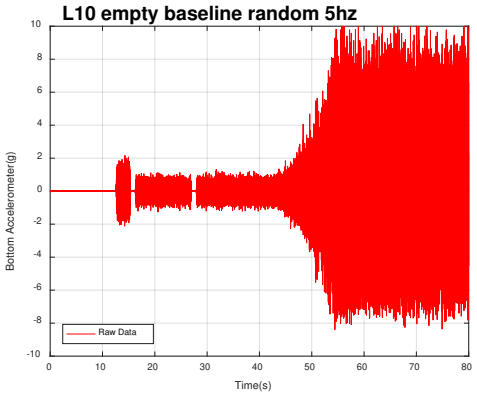

Empty Random

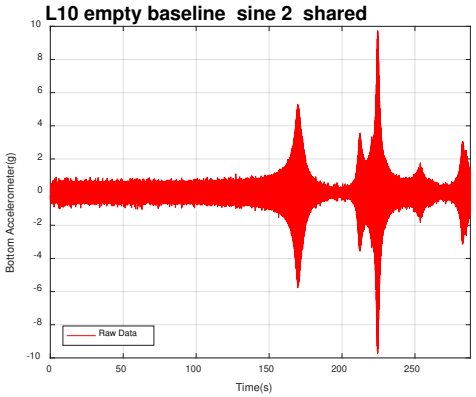

Empty Sine

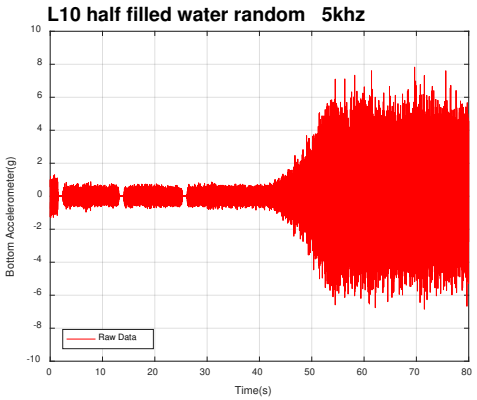

5L Water Random

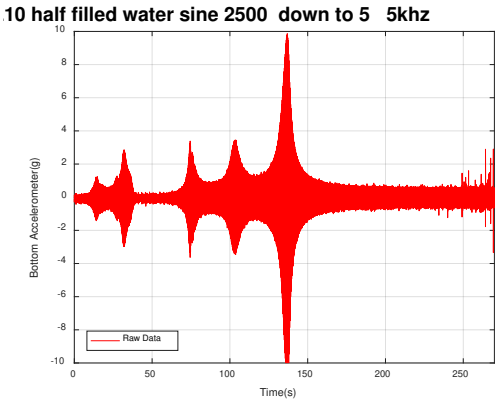

5L Water Sine

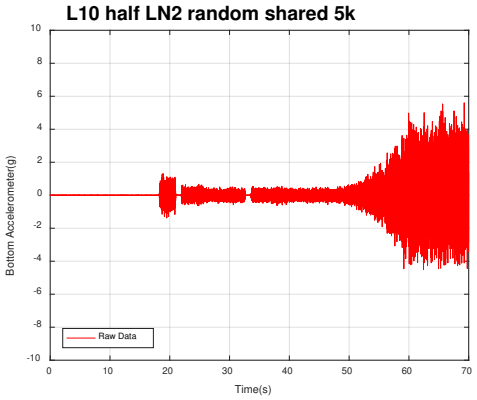

5L LN2 Random

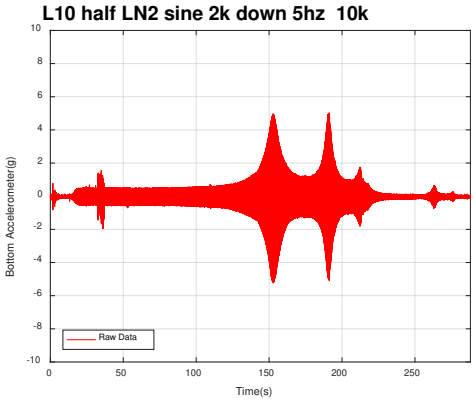

5L LN2 Sine

Figure 9 – Response Data

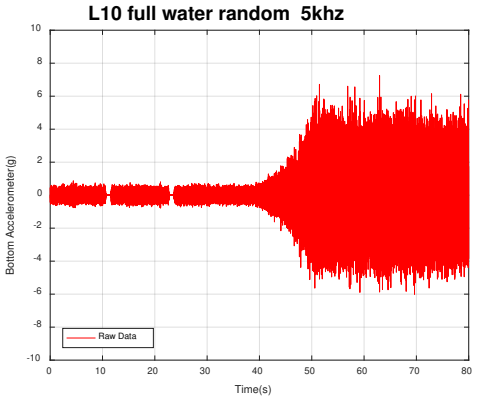

10L Water Random

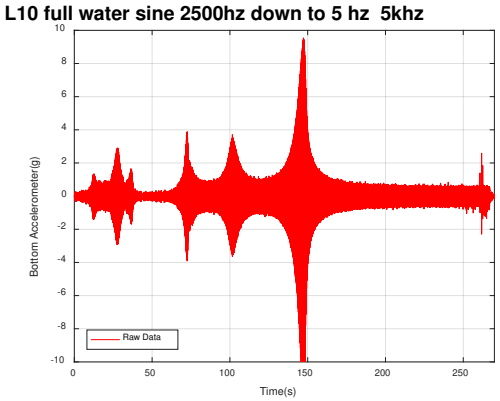

10L Water Sine

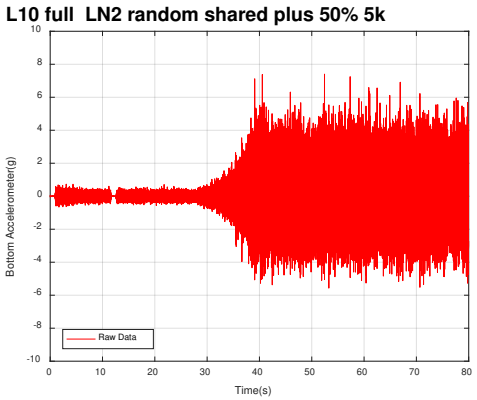

10L LN2 Random

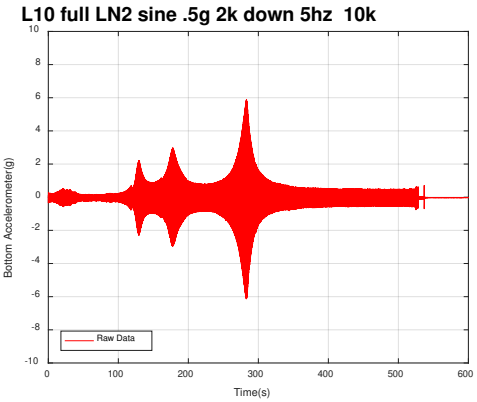

10L LN2 Sine (0.5 g)

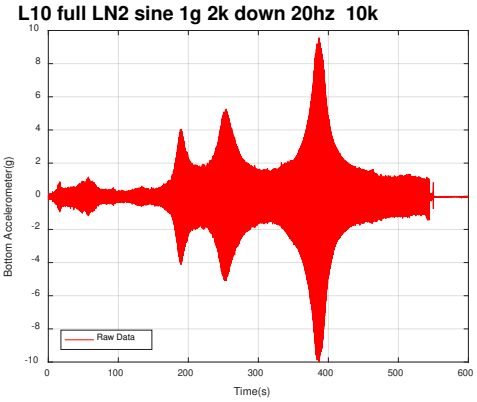

10L LN2 Sine (1 g)

Figure 10 – Response Data (continued)

Some initial observations can be made when comparing the raw response data gathered during each of the tests. For the random tests, graphing the amplitude of the response versus the test time shows the expected randomized response amplitudes. Because the sinusoidal tests swept through a steadily increasing or decreasing range of frequencies over time, the test time correlates to the frequency. As a result, plotting the amplitude over time for each of the sinusoidal sweep tests shows a few clear resonant frequencies. The results will have to be converted to a frequency response function before the frequency and amplitude of each resonant mode can be determined and the energy associated with each resonant mode can be calculated.

In addition, the sinusoidal sweep results also highlight areas of noise which have crept into the response data near the beginning or the end of each of the tests. One clear example can be seen in the graph of the response for the five liter water sine sweep test which shows narrow spikes in the data after approximately 260 seconds which do not appear to be associated with a resonance. The response of the random tests likely also have noise as well, however it is more difficult to see the spikes in the time domain due to the varied nature of the random response. This noise in the response signal is data that will have to be filtered when analyzing the results.

4.1.3. Filtering the Data

Noise is evident in the input and response data during the time of the sinusoidal sweep tests which corresponds to the higher frequencies. As a result, low-pass bandwidth filters shall be used to remove the noise from the signals before the data is used in calculations. The magnitude response diagram of the fifteenth order Butterworth filter used to clean up the input and response data is shown in Figure 11.

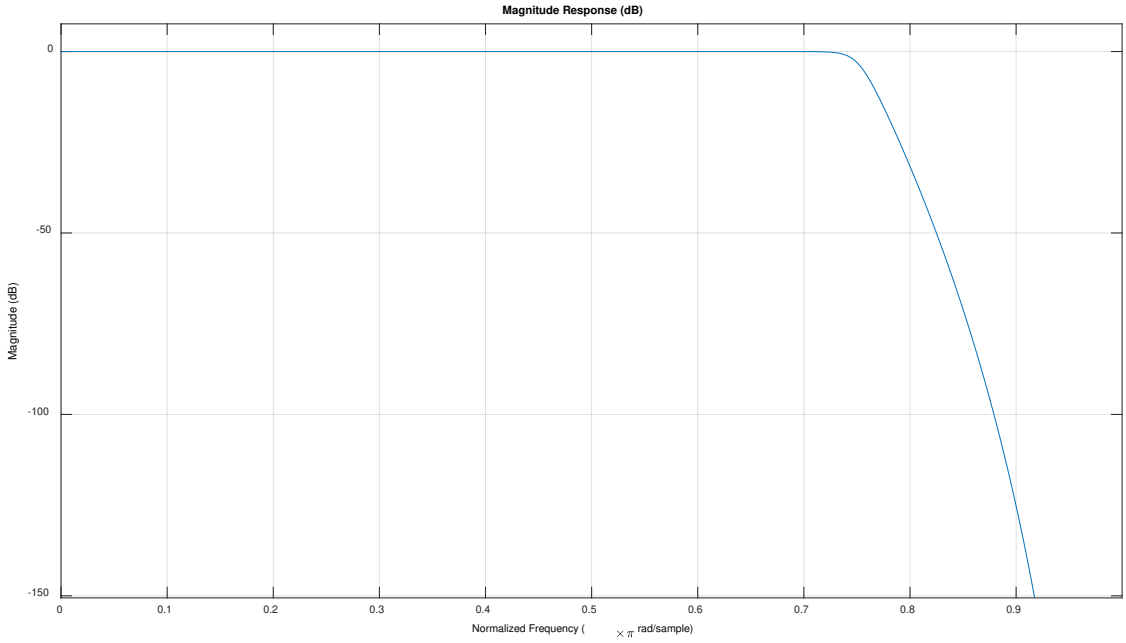

Figure 11 – Filter Visualization

Once the input and response data sets have been filtered, the data for each of the experiments is plotted again in the time domain. The filtered data is shown in blue and has been plotted concurrently with the original response data, in red, in order to highlight the noise which has been removed during the filtering process. These charts are given in Figure 12 and Figure 13.

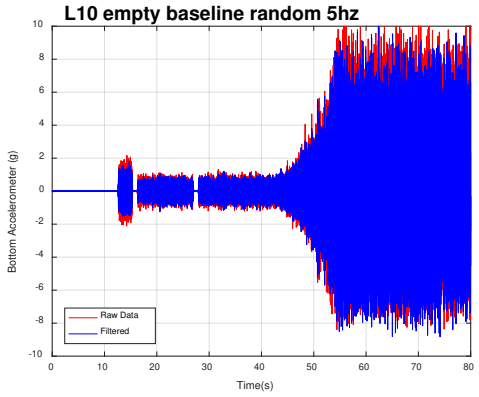

Empty Random

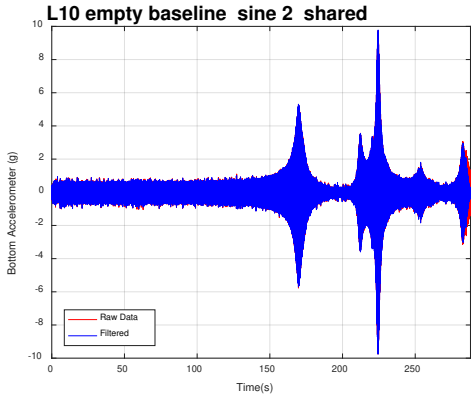

Empty Sine

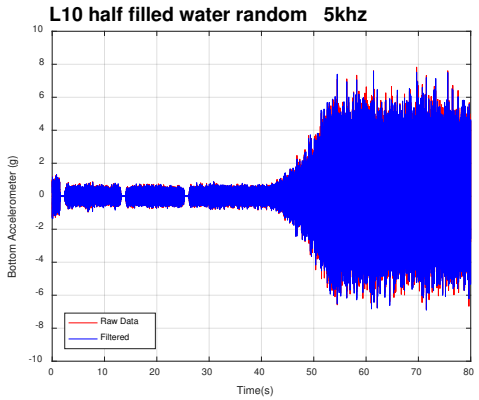

5L Water Random

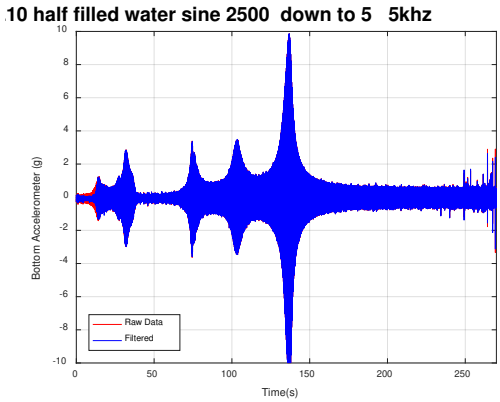

5L Water Sine

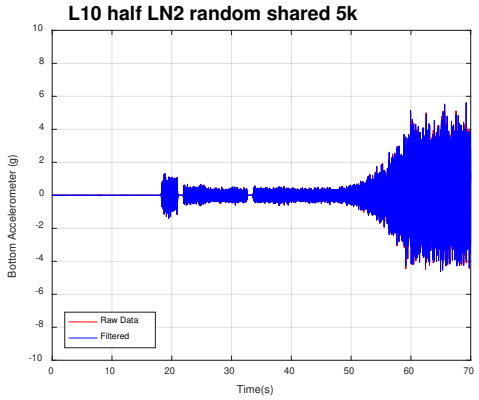

5L LN2 Random

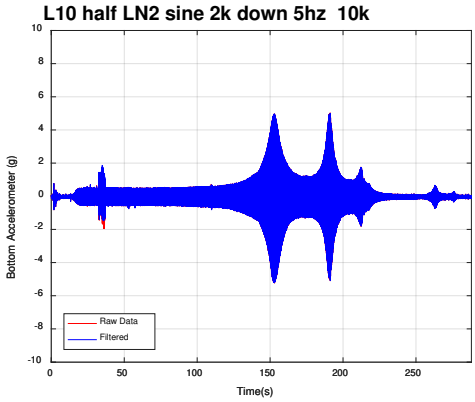

5L LN2 Sine

Figure 12 – Comparison of Raw and Filtered Response Data

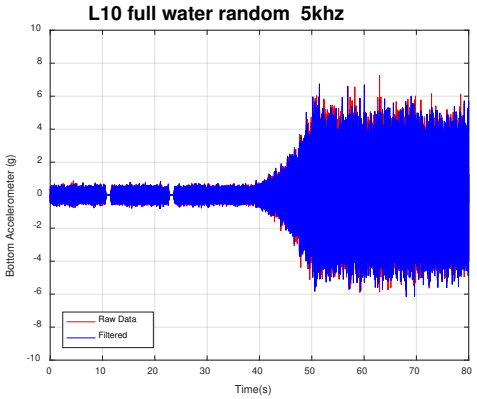

10L Water Random

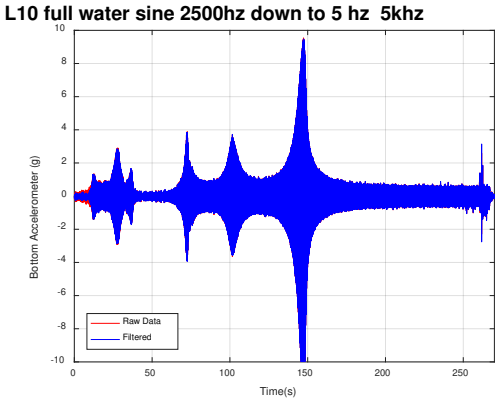

10L Water Sine

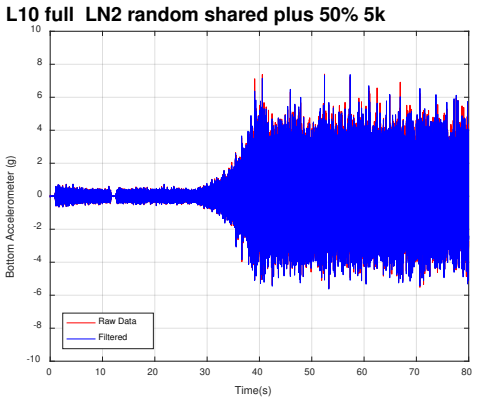

10L LN2 Random

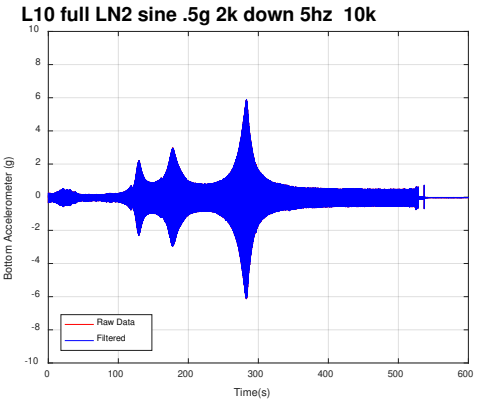

10L LN2 Sine (0.5 g)

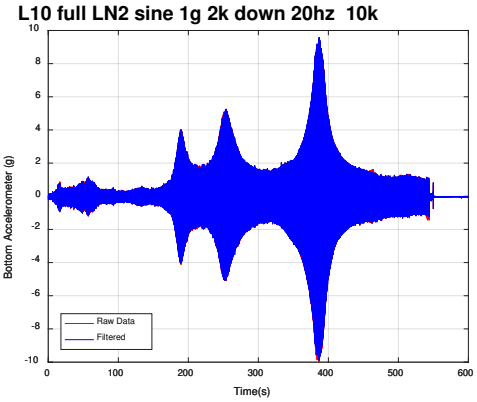

10L LN2 Sine (1 g)

Figure 13 - Comparison of Raw and Filtered Response Data (continued)

4.1.4. Creating Frequency Response Functions

Once the input and response data has been collected and the high-frequency noise has been filtered out, the data can then be used to create a frequency response function. The frequency response function is one of the most important representations of test data as it shows the frequencies at which each of the major modes for the system occurs and the maximum amplitude for each natural frequency. The frequency response function for each of the tests are shown in Figure 14 and Figure 15.

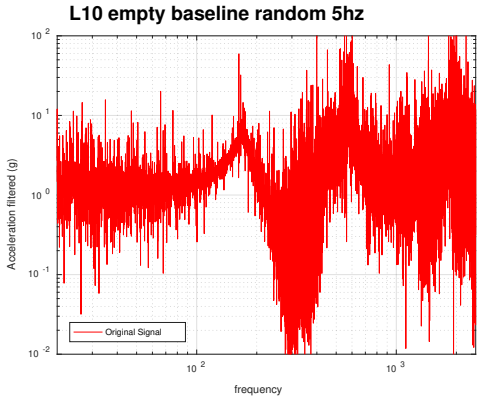

Empty Random

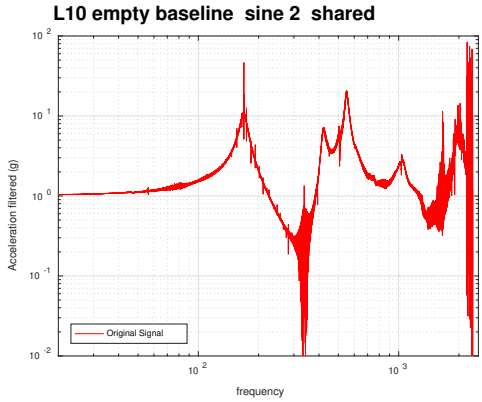

Empty Sine

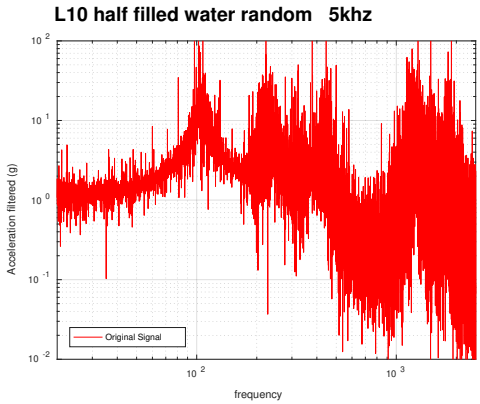

5L Water Random

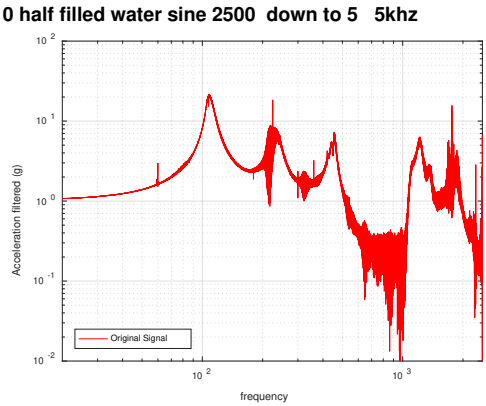

5L Water Sine

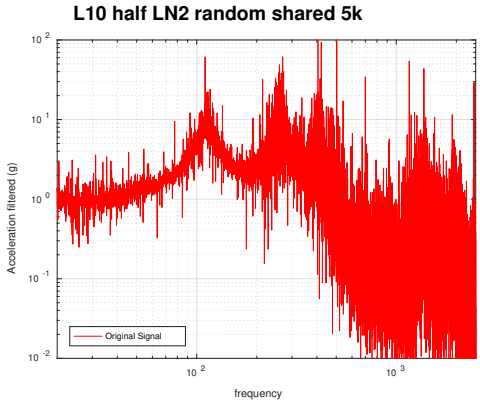

5L LN2 Random

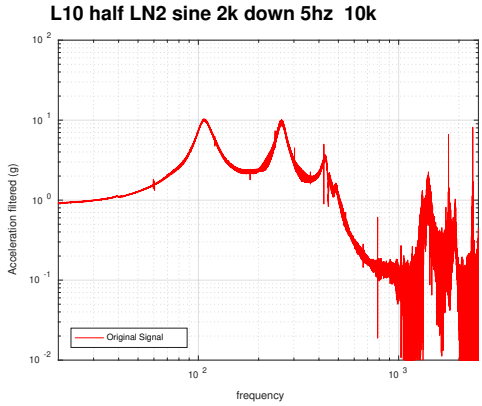

5L LN2 Sine

Figure 14 – Frequency Response Functions

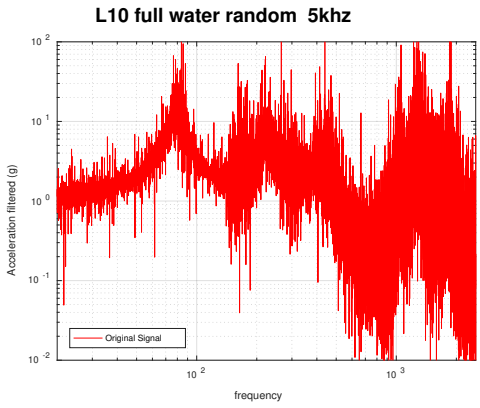

10L Water Random

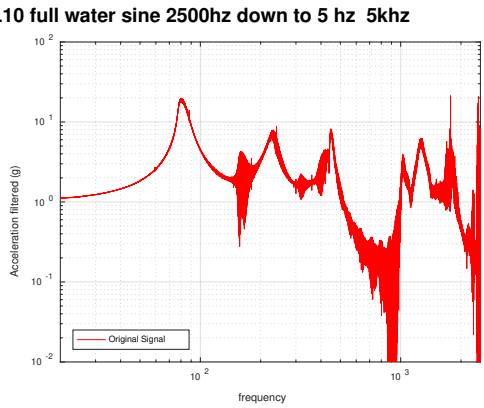

10L Water Sine

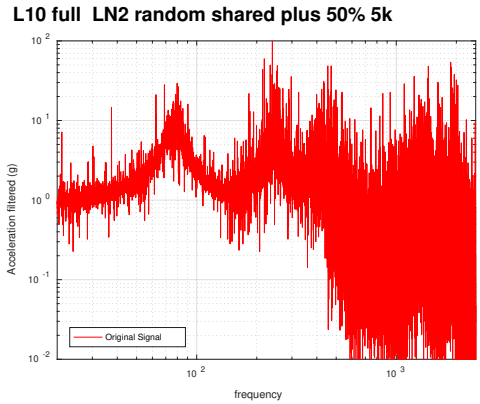

10L LN2 Random

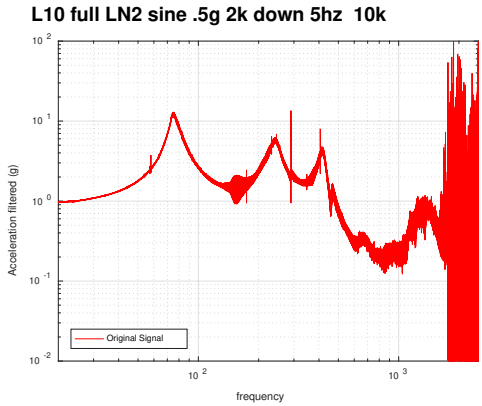

10L LN2 Sine (0.5 g)

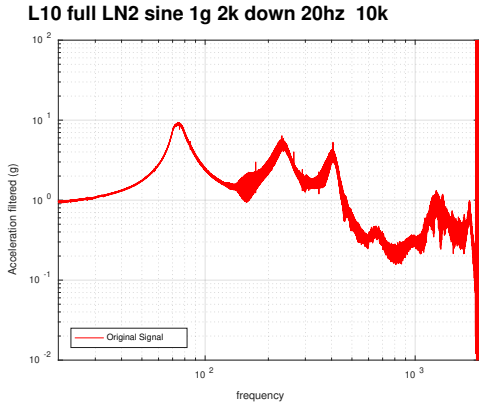

10L LN2 Sine (1 g)

Figure 15 - Frequency Response Functions (continued)

Despite the fact that some of the high frequency noise has been filtered out of the input data and the response data, there are still noisy spikes apparent in the frequency response curves. This is especially true in the FRFs for the random data; the noise makes the random data difficult to interpret. As a result, a second type of filter is used to clean up the frequency response function itself.

A third order, one-dimensional median filter is applied to the frequency response function; this filter uses a specified number of data points on either side of each data point and calculates the median amplitude to obtain the amplitude at each point. When there is a very high sampling rate and very narrow spikes in the data, as is the case here, the noise can be filtered out effectively using this filtering method without losing any of the essential amplitude or frequency values. The filtered and unfiltered FRFs have been plotted concurrently in Figure 16 and Figure 17, with the unfiltered data represented in red and the filtered FRF in blue.

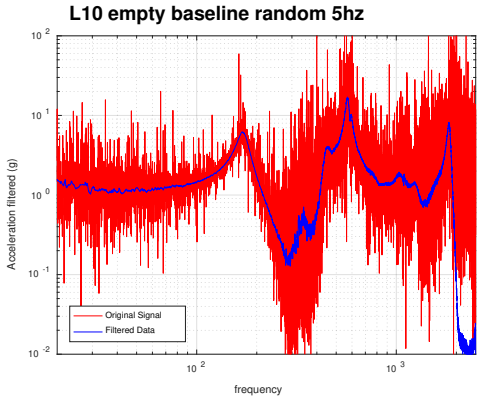

Empty Random

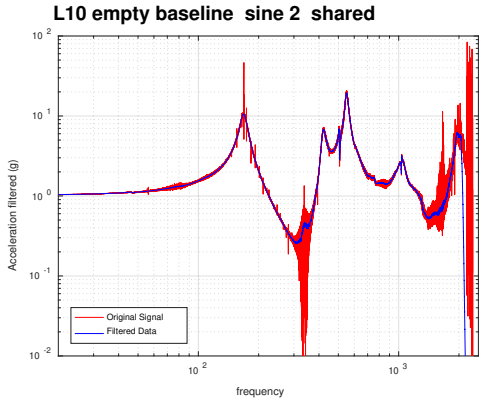

Empty Sine

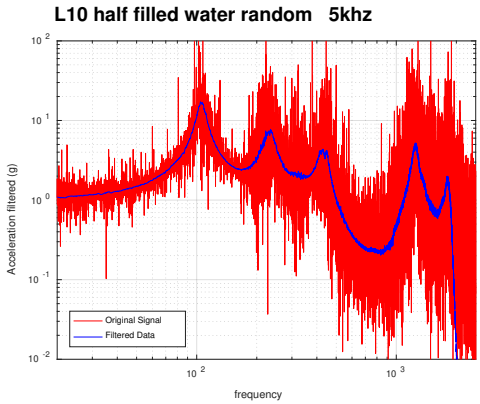

5L Water Random

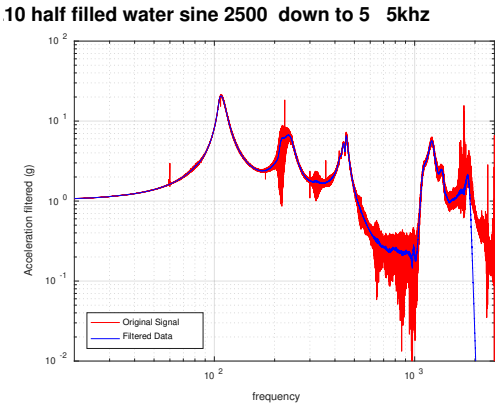

5L Water Sine

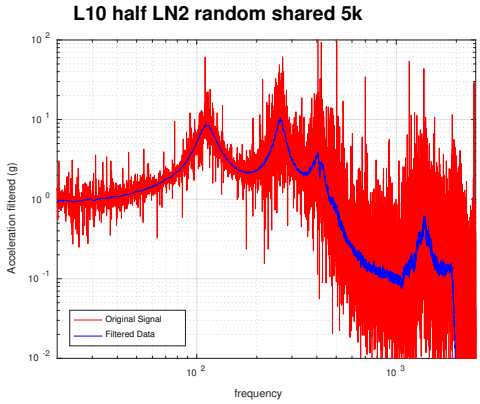

5L LN2 Random

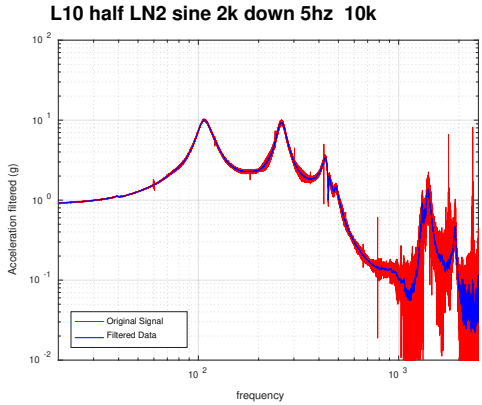

5L LN2 Sine

Figure 16 – FRF Comparison Between Filtered and Unfiltered

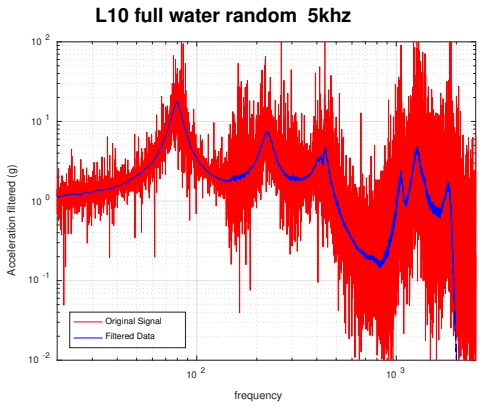

10L Water Random

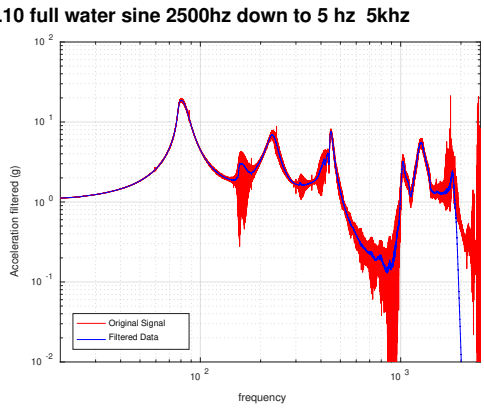

10L Water Sine

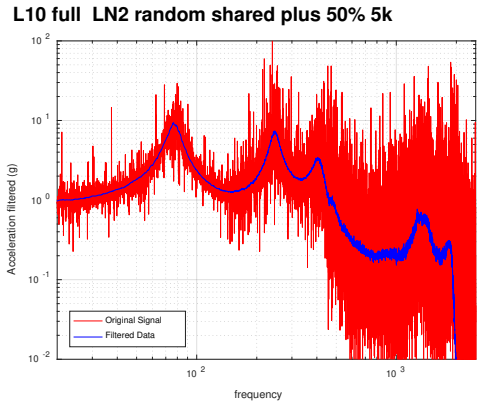

10L LN2 Random

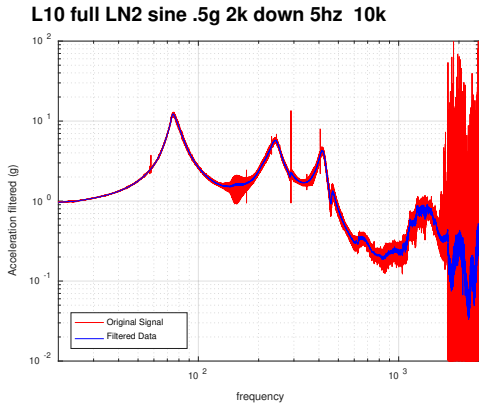

10L LN2 Sine (0.5 g)

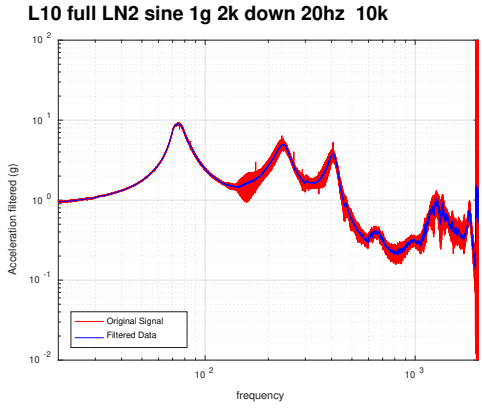

10L LN2 Sine (1 g)

Figure 17 - FRF Comparison Between Filtered and Unfiltered (continued)

By graphing the filtered and unfiltered data concurrently, it can be seen that the median filter has eliminated much of the unwanted noise in the FRF. Additionally, the FRFs for the random test and the sine test for each test set-up have been placed side by side in order to be able to compare the frequencies and the amplitudes between the two. As expected, whether the FRF was calculated using the data from the random test or from the sine sweep test, the frequency and amplitude associated with each of the major modes is nearly identical. Comparing the random and the sine results to each other for each type of tests confirms that the median filter did not compromise the essential amplitudes and frequencies of the major modes. The FRFs have been plotted again in Figure 18 and Figure 19 in order to show just the final, filtered frequency response function for each of the tests.

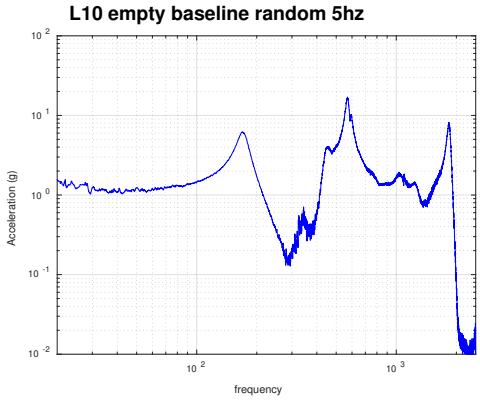

Empty Random

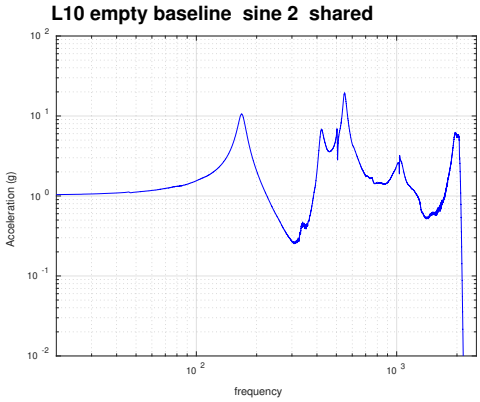

Empty Sine

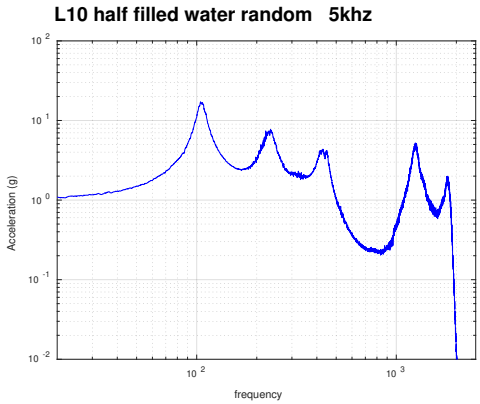

5L Water Random

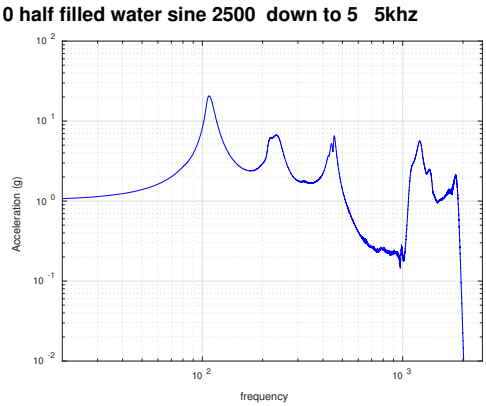

5L Water Sine

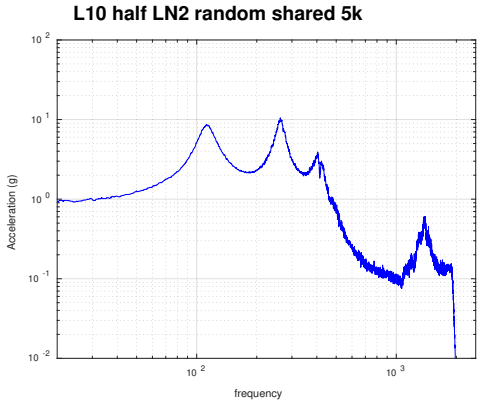

5L LN2 Random

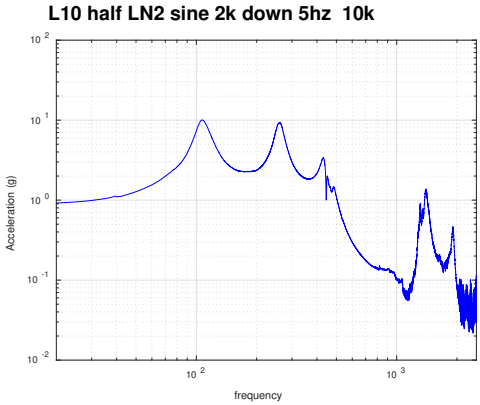

5L LN2 Sine

Figure 18 – Frequency Response Functions, Filtered

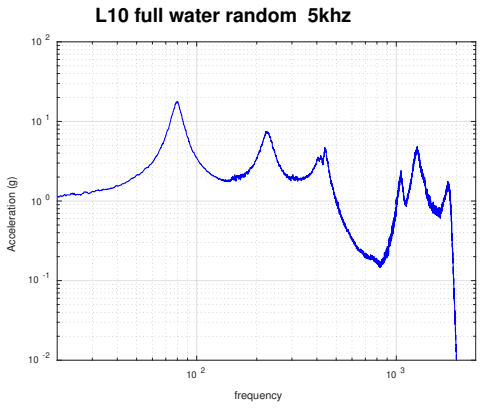

10L Water Random

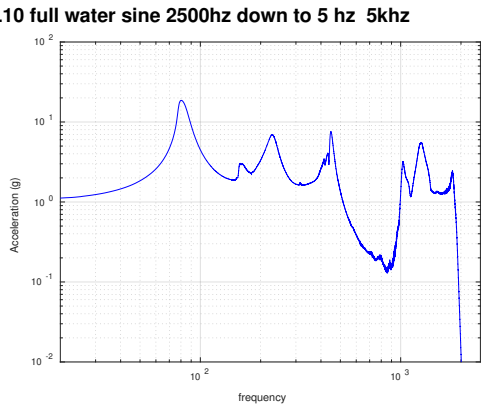

10L Water Sine

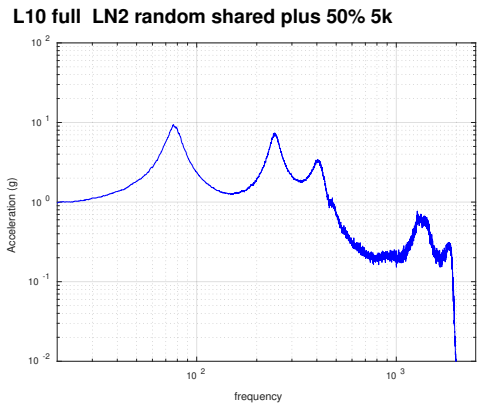

10L LN2 Random

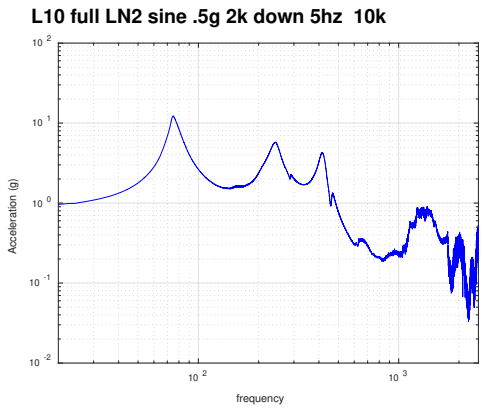

10L LN2 Sine (.5 g)

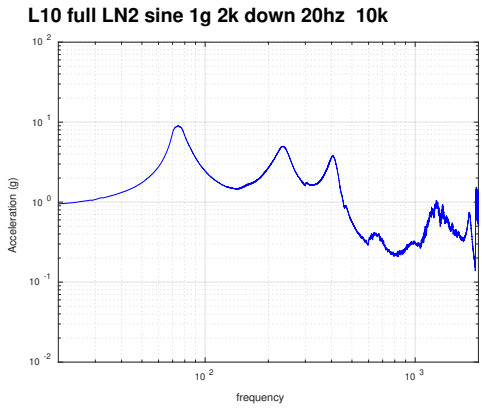

10L LN2 Sine (1 g)

Figure 19 - Frequency Response Functions, Filtered (continued)

4.1.5. Flow Meter Data

The rate of boil off of the liquid nitrogen was measured by sealing the neck of the storage container with a flow meter. During the second phase of testing, the resting rate of boil off of the fluid was measured at 7.0 liters per minute. The tests in which the tank was vibrated empty or filled with water, no significant data was gathered from the flow meter as was expected due to the fact that water does not boil off at room temperature as liquid nitrogen does.

A summary of the flow meter data for the five liquid nitrogen tests is given in Figure 20; the flow meter data is shown in blue while the response data has been overlaid in red. This was done to highlight the correlation between the resonant frequencies of the system and the increased rates of boil off.

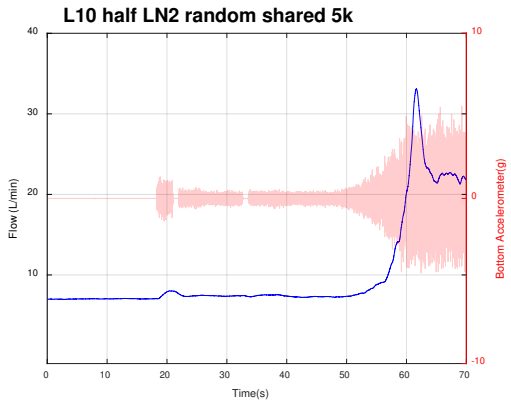

5L LN2 Random

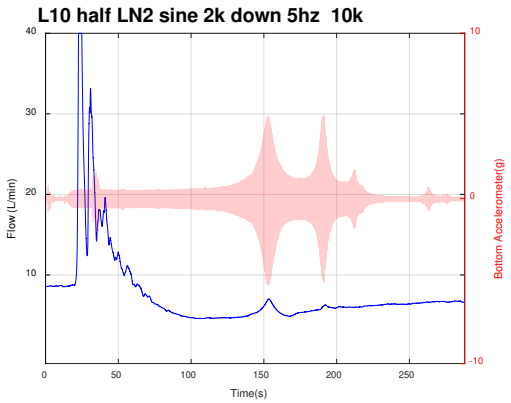

5L LN2 Sine

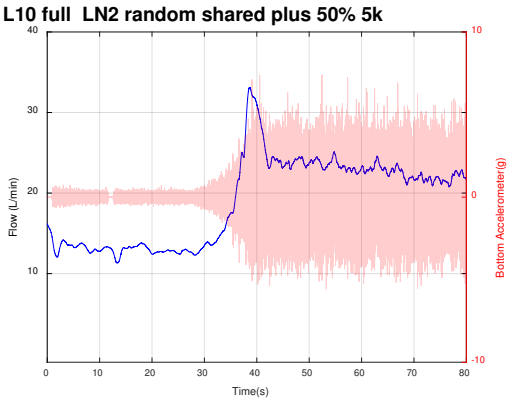

10L LN2 Random

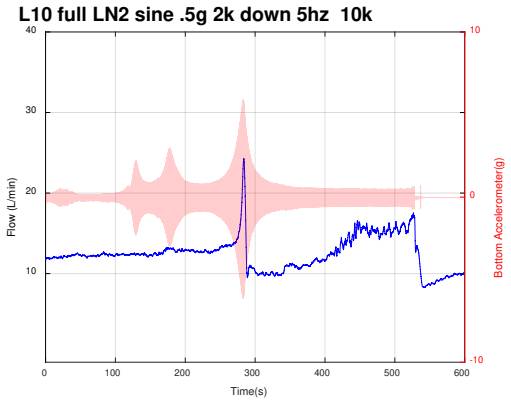

10L LN2 Sine (0.5 g)

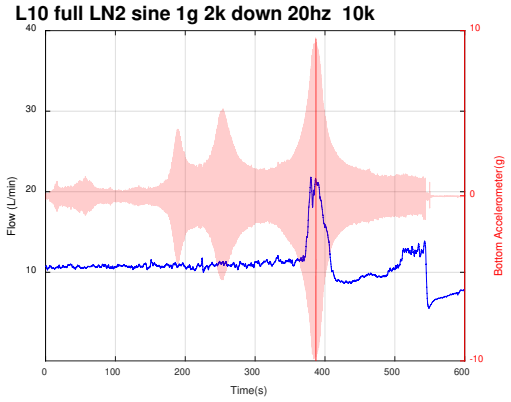

10 LN2 Sine (1 g)

Figure 20 – Flow Meter Data Overlaid with Response Data

It is immediately obvious that for each liquid nitrogen test, the rate of boil-off did measurably increase under the application of vibration to the system. For the random five liter test, the rate of vapor exiting the system maintained a steady state rate of approximately 7 liters per minute while the system was at rest and while the shaker table ramped up to full amplitude. Once the full level of vibration was achieved approximately sixty seconds into the test, the flow rate spiked to 33 liters per minute, increasing nearly 4.7 times above the resting rate before dropping down to a steady rate of 22 liters per minute, an increase of over 3 times the resting rate for the remainder of the test. The second random test showed a similar pattern, maintaining an initial flow rate of approximately 12 liters per minute while the system ramped up to full random amplitude, spiking up to 33 liters per minute, increasing nearly 4.75 times over the resting rate once full amplitude random vibration was achieved, and then dropping to a steady rate of 23 liters per minute, maintaining an increase of 3 times the resting rate for the remainder of the test.

During each of the two sine tests in which the tank was filled with ten liters of liquid nitrogen, the rate of boil off maintained a steady state of approximately 11 to 12 liters per minute until the system neared its resonant frequencies. Once the largest major resonant frequency was achieved by the system, the rate of boil off increased to approximately 22 to 24 liters per minute; increasing approximately 3 times the resting flow rate.

For the third sine sweep test, the one in which the tank was filled with five liters of liquid nitrogen, the correlation between the flow meter readings and the resonant frequencies of the system is less pronounced. The flow rate spiked early in the test, before the shaker table had neared any of the resonant frequencies of the system. The flow rate did rise again as the system neared its two major resonant frequencies, but not significantly enough to yield useful data for the purposes of this analysis. It is possible that the flow meter data was corrupted; either by the flow

meter being improperly attached, allowing a leak of nitrogen vapor, or possibly by the liquid nitrogen splashing inside the tank.

For each test, the flow meter recorded an initial flow rate, a spike corresponding to either ramp up of the random vibration or a resonant frequency in the sine tests, followed by new steady state flow rate which was higher than the resting rate but less than the maximum peak rate. A summary of the peak flow rates and the elevated steady state flow rate for each of the five liquid nitrogen test configurations is given in Table 6. Also given is the factor of increase of the peak flow over the resting flow rate of 7 liters per minute.

Table 6 – Maximum Flow Rate

		Peak (L/min)	Factor of Increase Over Resting Rate	Elevated Steady State (L/min)	Factor of Increase Over Resting Rate
Sine	5L LN2 *	40.00	5.7	6	-0.1
	10L LN2 (.5 g)	24.27	3.5	17	2.4
	10L LN2 (1g)	21.82	3.1	12	1.7
Random	5L LN2	33.11	4.7	22	3.1
	10L LN2 (.5 g)	33.12	4.7	22	3.1

* flow meter data inconsistent

4.2. Analysis

4.2.1. Calculating Mechanical Energy Absorbed

Now that the frequency response function for each experiment has been calculated and the noise has been filtered out of the response data, the frequency and amplitude associated with each of the major modes can be determined and used to calculate the energy of the system. The filtered frequency response function for the ten liter liquid nitrogen (.5 g) test is shown again in Figure 21.

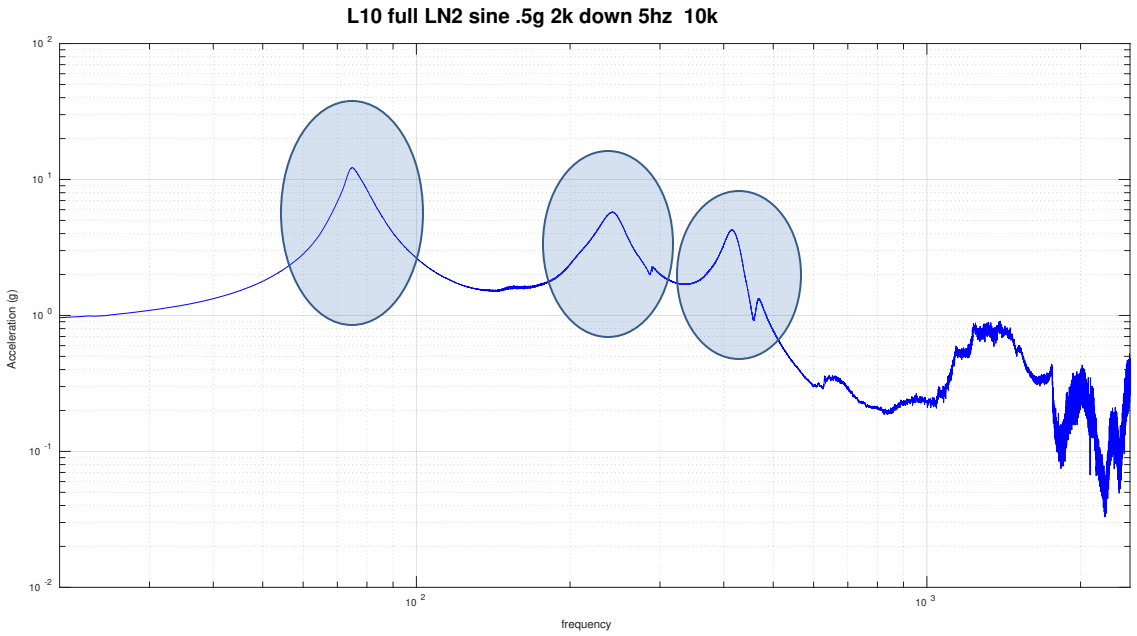

Figure 21 – Frequency Response Function for 10L LN2 (.5 g) Test

There are three major modes apparent for this test, highlighted in blue, with the first mode occurring between 70 and 80 Hz, the second between 200 and 300 Hz and the third major mode occurring between 400 and 500 Hz. Any other modes beyond these first three major modes can

be considered negligible and shall be ignored for the purposes of calculating the energy of the system. The same concept is applied for all eleven tests; the first three major modes are retained and any other modes are considered to be negligible and are not included in the subsequent energy calculations.

The graphs shown in Figure 22 show a close up of the FRF for each of the three major modes for the ten liter liquid nitrogen (.5 g) test. In addition, the half-power bandwidth frequencies have been calculated and the corresponding horizontal line is shown on the graph for each mode. Where this line first crosses the FRF, to the left of the peak, is the lower half-power bandwidth frequency (f_a) and where the line crosses the FRF again, to the right of the peak, is the upper half-power bandwidth frequency (f_b).

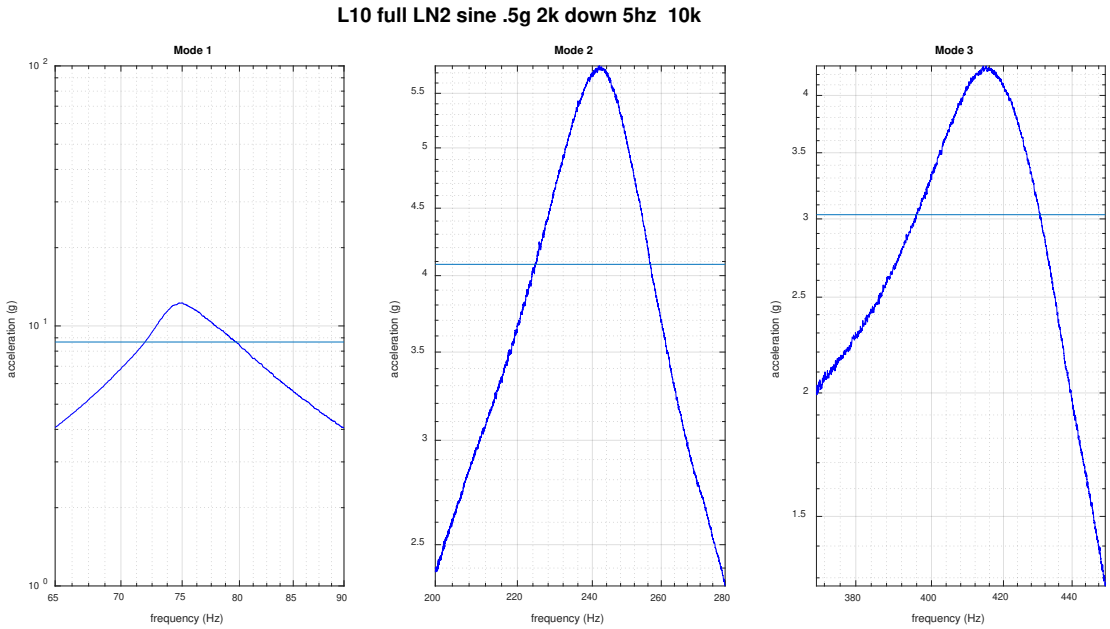

Figure 22 – Closeup of Major Modes for 10L LN_2 (.5 g) Test

A summary of the frequencies for first three major modes (f_r), the lower and upper half-power bandwidth frequencies (f_a and f_b), and the corresponding magnitudes (A_{max}) are listed in Table 7 for each of the random tests and in Table 8 for each of the sine swept tests.

Table 7 – Major Modes for Random Tests

Test Description	Major Mode	Resonant Frequency f_r (Hz)	Half-power bandwidth f_a (Hz)	Half-power bandwidth f_b (Hz)	Amplitude (g)
Empty Baseline Random	1	170.2	158.5	180.4	6.2
	2	569.3	557.8	580.1	17.0
	3	1838.4	1804.1	1880.4	8.7
5L Water Random	1	104.6	100.6	111.2	17.1
	2	234.5	217.1	245.6	7.7
	3	429.0	399.4	456.2	4.4
5L LN2 Random	1	111.6	103.2	122.5	8.6
	2	569.3	557.8	272.1	10.5
	3	404.0	388.6	421.1	3.4
10L Water Random	1	79.6	75.9	83.6	17.8
	2	223.3	213.2	239.1	7.5
	3	438.0	413.1	449.3	4.7
10L LN2 Random	1	76.6	72.0	82.8	9.3
	2	245.2	233.7	259.0	7.4
	3	403.6	377.6	426.4	3.4

Table 8 – Major Modes for Sine Sweep Tests

Test Description	Major Mode	Resonant Frequency f_r (Hz)	Half-power bandwidth f_a (Hz)	Half-power bandwidth f_b (Hz)	Amplitude (g)
Empty Baseline Sine Sweep	1	168.1	161.3	175.2	10.6
	2	550.5	539.5	560.9	6.7
	3	1963.9	1918.1	2055.6	6.3
5L Water Sine Sweep	1	107.9	104.3	113.6	20.7
	2	233.6	211.9	248.8	6.7
	3	455.9	435.8	464.4	6.5
5L LN2 Sine Sweep	1	107.0	99.6	116.2	10.1
	2	260.8	246.8	273.3	9.3
	3	428.8	407.8	440.2	3.4
10L Water Sine Sweep	1	80.3	77.2	86.2	18.6
	2	229.2	213.9	241.7	7.0
	3	448.1	442.3	458.6	7.6
10L LN2 Sine Sweep 0.5 g	1	75.0	71.9	79.7	12.3
	2	242.0	224.5	256.6	5.8
	3	414.2	295.8	430.6	4.3
10L LN2 Sine Sweep 1.0 g	1	74.4	69.1	80.6	9.1
	2	235.8	214.2	253.0	5.0
	3	405.6	383.3	423.5	3.8

Using the Half-Power Bandwidth Method, the rate of energy absorbed at each of the first three major modes of the system can now be calculated. This is repeated for each of the eleven tests in order to determine the total energy absorbed for each system. Recall that the Q-factor is a representation of the damping of the system at a particular mode; a large Q-factor represents low damping and a small Q-factor represents high damping. A list of the resonant frequencies, the displacements at each frequency, the Q-factors and the calculated total energy of the system (W) is given in Table 9 through Table 13.

Table 9 - Q-Factor and Energy – Empty

	Empty Baseline Random				**Empty Baseline Sine**			
Mode	f_r (Hz)	X (m)	Q	W (kW)	f_r (Hz)	X (m)	Q	W (kW)
1	170.2	0.0931	7.8	4,012.7	168.1	0.0931	12.1	2,492.4
2	569.3	0.0058	25.5	180.3	550.5	0.0058	25.7	161.7
3	1838.4	0.0013	24.1	294.2	1963.9	0.0013	14.3	605.1
	Total Energy		(W_{tot})	4,487.2	Total Energy		(W_{tot})	3,259.2

Table 10 - Q-Factor and Energy – 5 L Water

	5L Water Random				5L Water Sine			
Mode	f_r (Hz)	X (m)	Q	W (kW)	f_r (Hz)	X (m)	Q	W (kW)
1	104.6	0.1445	9.8	3,282.4	107.9	0.1445	11.6	3,048.3
2	234.5	0.0314	8.2	2,085.3	233.6	0.0314	6.3	2,679.6
3	429.0	0.0236	7.5	7,850.9	448.1	0.0236	15.9	4,465.1
	Total Energy		(W_{tot})	13,218.6	Total Energy		(W_{tot})	10,193.0

Table 11 - Q-Factor and Energy – 5 L LN_2

	5L LN_2 Random				5L LN2 Sine			
Mode	f_r (Hz)	X (m)	Q	W (kW)	f_r (Hz)	X (m)	Q	W (kW)
1	111.6	0.2155	5.8	13,727.0	107.0	0.2155	6.4	10,863.4
2	262.6	0.0367	14.7	2,044.8	260.8	0.0367	9.8	2,995.5
3	404.0	0.0047	12.4	146.7	428.8	0.0047	13.2	165.0
	Total Energy		(W_{tot})	15,918.5	Total Energy		(W_{tot})	14,024.0

Table 12 - Q-Factor and Energy – 10 L Water

	10L Water Random				10L Water Sine			
Mode	f_r (Hz)	X (m)	Q	W (kW)	f_r (Hz)	X (m)	Q	W (kW)
1	79.6	0.2998	10.4	8,593.3	80.3	0.2998	8.9	10,238.7
2	223.3	0.0350	8.6	3,117.1	229.2	0.0350	8.2	3,528.7
3	438.0	0.0236	12.1	7,627.1	448.1	0.0236	27.4	3,598.1
	Total Energy		(W_{tot})	19,337.4	Total Energy		(W_{tot})	17,365.5

Table 13 - Q-Factor and Energy – 10 L LN_2

	10L LN_2 Random				**10L LN2 Sine (.5 g)**			
Mode	f_r (Hz)	X (m)	Q	W (kW)	f_r (Hz)	X (m)	Q	W (kW)
1	76.6	0.1957	7.1	4,196.1	75.0	0.1957	9.6	2,908.7
2	245.2	0.0253	9.7	1,690.9	242.0	0.0253	7.5	2,088.5
3	403.6	0.0171	8.3	4,016.9	414.2	0.0171	11.9	3,014.4
	Total Energy		(W_{tot})	9,903.8	Total Energy		(W_{tot})	8,011.6

10L LN2 Sine (1 g)

Mode	f_r (Hz)	X (m)	Q	W (kW)
1	74.4	0.0551	6.5	336.3
2	235.8	0.0360	6.1	4,836.6
3	405.6	0.0159	10.1	2,893.7
	Total Energy		(W_{tot})	8,066.5

The total energy absorbed by each system is simply the sum of the energy for each of the three major modes. The total energy for each of the sine tests and the random tests is given in Figure 23.

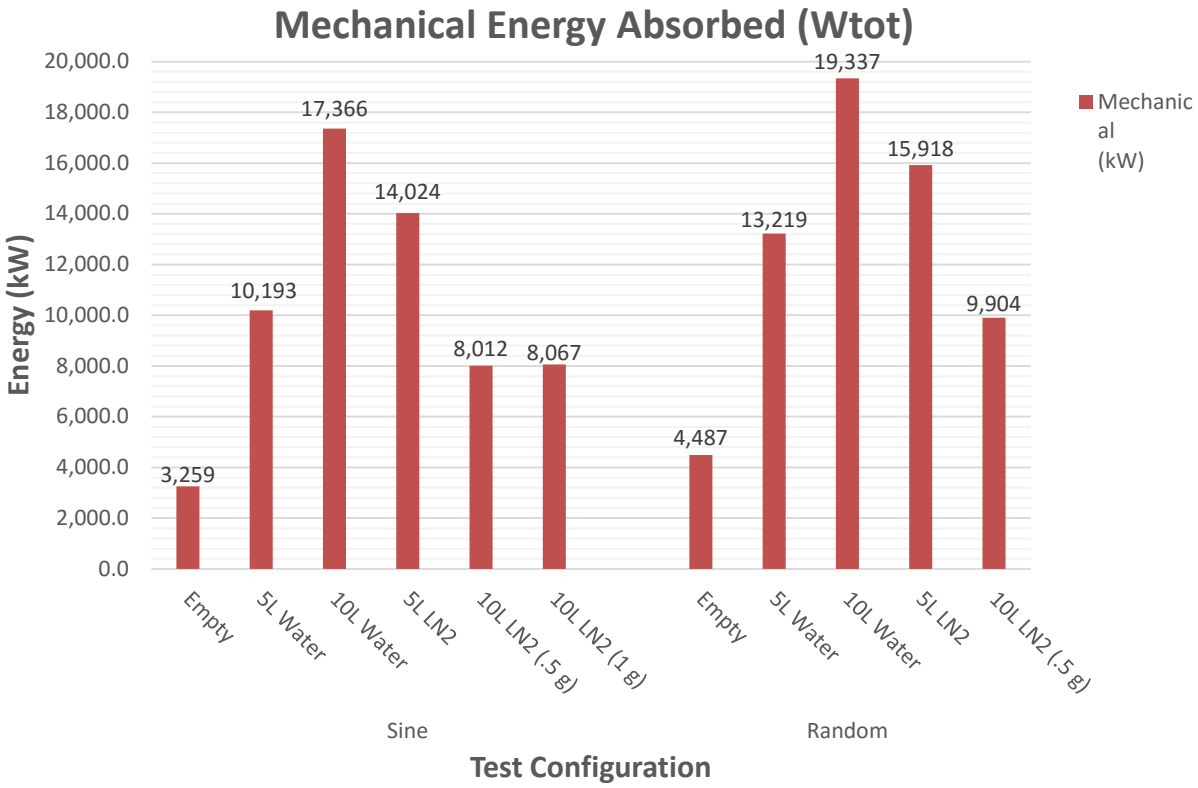

Figure 23 – Summary of Total Mechanical Energy Absorbed by System (W_{tot})

Note that the energy absorbed for each test configuration was comparable whether it was derived using the random test data or the sine test data. The empty tank configuration absorbed the least energy because the tank had no fluid inside it to create viscous damping. The five liter and ten liter water tests each absorbed successively more energy due to the increased damping effect of the volume of water inside the tank. While the five and ten liter liquid nitrogen tests did also absorb more energy than the empty tank test, unlike the water tests, the five liter liquid nitrogen test actually absorbed more mechanical energy than the ten liter test did. This is most likely due to the effect of boil off of the cryogenic fluid; more of the total energy of the ten liter system was lost in the form of thermal energy as more of the liquid nitrogen evaporated.

4.2.2. Calculating Thermal Energy Lost

In order to calculate the total thermal energy lost by the system during each test, the energy at each increment of time is calculated first and then the incremental energies are summed up in order to find an accurate representation of the total energy lost by the system.

The thermal energy lost by the system for each test is listed in Table 14. Also listed is the total theoretical resting thermal energy; this is the thermal energy that would have been lost to boil off of the cryogenic fluid with each system completely at rest over the same period of time.

Table 14 –Thermal Energy Lost by Systems

		Actual (kJ)	Theoretical (kJ)	Factor of Increase
Sine	5L LN2	5,930.1	5,627.7	1.1
	10L LN2 (.5 g)	20,041.0	11,255.4	1.8
	10L LN2 (1g)	17,381.0	11,255.4	1.5
Random	5L LN2	1,884.1	1,313.1	1.4
	10L LN2 (.5 g)	4,077.5	1,500.7	2.7

The plot in Figure 24 shows the total thermal energy lost over the entire duration of each test. In addition to the actual loss of energy calculated using the flow meter data, the total theoretical amount of energy which would have been lost with the system at rest for the same amount of time is displayed as well.

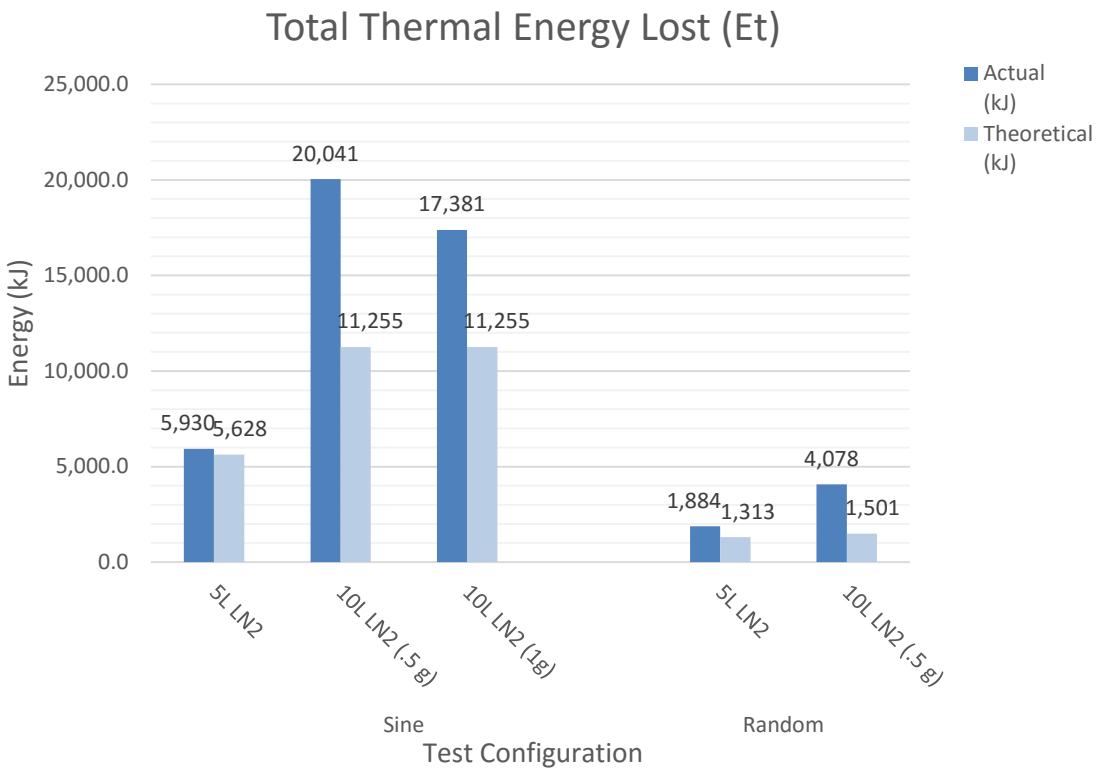

Figure 24 – Total Thermal Energy Lost (E_t)

The random tests were only 70 to 80 seconds long, so the total amount of nitrogen vapor to exit the system during that time would be the smallest for the random tests. The five liter tests were 300 seconds each allowing the total amount of thermal energy lost by the system would increase, and the ten liter tests were 600 seconds each, which accounts for the high total thermal energy losses of those systems.

Recall that the flow meter data recorded for the five liter liquid nitrogen sine sweep test was inconsistent with expectations. The spikes in the rate of flow occurred very early in the test and the data did not significantly spike again near the resonant frequencies. As a result, the calculated thermal energy lost for that test also appears to be out of family. For each of the other

random and sine sweep tests, the system lost 40 to 170% more thermal energy during the vibrational testing than the total theoretical energy loss if the system had been at rest. However the five liter sine sweep system only lost 5% more energy than it would have at rest. This is further evidence that the flow meter data from that test may be inaccurate.

The actual thermal energy lost during a test should exceed the theoretical resting value because as the system experiences vibration which causes an increased rate of boil off, the flow rate should also be elevated as well.

The rate of thermal energy lost by each system is listed in Table 15.

Table 15 –Thermal Energy Lost by Systems

		Average Rate of Energy Loss (kW)	Peak Rate of Energy Loss (kW)	Theoretical Rate of Energy Loss (kW)	Factor of Increase (Average)	Factor of Increase (Peak)
Sine	5L LN2	59.0	107.2	18.8	3.1	5.7
	10L LN2 (.5 g)	38.6	65.0	18.8	2.1	3.5
	10L LN2 (1g)	32.7	58.5	18.8	1.7	3.1
Random	5L LN2	50.2	88.7	18.8	2.7	4.7
	10L LN2 (.5 g)	56.8	88.8	18.8	3.0	4.7

4.2.3. Total Energy

The total energy is calculated by adding the total thermal energy lost and the total mechanical energy absorbed. The total energy for each sine sweep test is listed in Table 16 and the total for each random test is listed in Table 17.

Table 16 –Energy Loss Rate (Sine Sweep Tests)

	Test Configuration	Mechanical, W_{tot} (kW)	Thermal, E_t (kW)
Sine	Empty	3,259.2	
	5L Water	10,193.0	
	10L Water	17,365.5	
	5L LN2	14,024.0	59.0
	10L LN2 (.5 g)	8,011.6	38.6
	10L LN2 (1 g)	8,066.5	32.7

Table 17 – Energy Loss Rate (Random Tests)

	Test Configuration	Mechanical, W_{tot} (kW)	Thermal, E_t (kW)
Random	Empty	4,487.2	
	5L Water	13,218.6	
	10L Water	19,337.4	
	5L LN2	15,918.5	50.2
	10L LN2 (.5 g)	9,903.8	56.8

CHAPTER 5

CONCLUSION

5.1. Conclusion

The loss of cryogenic fluids due to boil-off did, in fact, increase during the application of mechanical energy to the cryogenic storage system. During vibrational testing, the rate of boil off of the liquid nitrogen peaked 3.1 to 4.7 times higher than the resting rate of boil off. After the peak flow rate passed, the vibrating systems still maintained a steady elevated flow rate 1.7 to 3.1 times over the resting flow rate for the remainder of the vibration test. As viscous damping of the fluid caused the cryogen to boil off at an increased rate, the total amount of thermal energy lost by each of the liquid nitrogen tests increased on average by a factor of 1.1 to 2.7 times above the total theoretical resting thermal energy loss as well.

Mechanical energy applied to the system in the form of vibrational energy is converted into thermal energy via viscous damping of the fluid. Current storage systems include advanced thermal insulation systems to mitigate the loss of cryogenic fluids due to thermal conduction. However, it may be possible to increase the efficiency of cryogenic storage systems with the addition of mechanical damping to reduce the vibrational energy entering the system during transport, storage or during a launch.

APPENDIX

MATLAB PROGRAM

```
%%Erin Schlichenmaier - Matlab code for thesis
%THE EFFECT OF VIBRATION ON CRYOGENS BOIL-OFF DURING LAUNCH, TRANSFER
%AND TRANSPORT
clear all; close all;  clc; format compact;

%%%%%% SINE GRAPHS 1 g %%%%%%
%%%%%ENTER FILENAME%%%%%%%%%%
file='C:\Users\Erin\Documents\Erin\Cryo Project\Matlab\Test 3\L10 full LN2
sine 1g 2k down 20hz  10k.mat';
filename='L10 full LN2 sine 1g 2k down 20hz  10k';
Vib=load(file);
numpoints=max(size(Vib.ch0a_dataa));

%%%%%ENTER DATA%%%%%%%%%%%%%%%
    t_n=600;                %total time of test in seconds
    sensitivity=10;         %sensitivity adjustment
    freqmin=20;             %min frequency of test in Hz
    freqmax=2000;           %max frequency of test in Hz
    Wn= .75;                %cutoff frequency for butterworth filter
    order=15;               %order of butterworth filter
    mass=13.982;            %mass of filled container in kg
%first mode frequency range     %first mode time range
    minimum1=50;               tmode11=120;
    maximum1=110;               tmode12=140;
%second mode frequency range    %second mode time range
    minimum2=150;              tmode21=150;
    maximum2=300;              tmode22=200;
%third mode frequency range     %third mode time range
    minimum3=300;              tmode31=250;
    maximum3=500;              tmode32=300;
%Some stuff I need for later
    dt=t_n/numpoints;          Fs=1/dt;
    N=(1/dt)/2;                g=9.80665;
    SM_No=numpoints;           L=SM_No/2;
    hVap=199;                  rho=808;
%input equation
    t=linspace(0,t_n,numpoints);
    input=freqmax*exp(-.007675*t);

%%%%%%%%%%%%%%%%%%%%%%%%%%%%%%%%%%%%%%%%%%%%%%%%%%%%%%%%%%%%%%%%%%%%%%%%%%%%
%%%%%%%%%%%%%%%%%%%%%%%%%%%%%%%%%%%%%%%%%%%%%%%%%%%%%%%%%%%%%%%%%%%%%%%%%%%%
%Apply factor to scale data properly
ch0=Vib.ch0a_dataa*sensitivity;
ch1=Vib.ch1a_dataa*sensitivity;
ch2=Vib.ch2a_dataa*sensitivity;
ch3=Vib.ch3a_dataa;
ch4=(Vib.ch4a_dataa*4);                %convert to liters per minute

%Start by designing filter.
[b,a]=butter(order,Wn);
y=filter(b,a,ch0);
y1=filter(b,a,ch1);
```

```
%%%%%%%%%%%%%%%%%%%%%%%%%%%%%%%%%%%%%%%%%%%%%%%%%%%%%%%%%%%%%%%%%%%%%%%%%%%%
%Plot just the raw input data
figure(1);              plot(t,ch1,'r');
xlabel('Time(s)');      ylabel('Load Cell(g)');
xlim([0 t_n]);          ylim([-5 5]);
grid on;                legend('Raw Data','Location','SouthWest')
set(gcf,'NextPlot','add');
axes; h = title(filename,'FontSize', 20);
set(gca,'Visible','off'); set(h,'Visible','on');

%Plot just the raw response data
figure(2);              plot(t,ch0,'r');
xlabel('Time(s)');      ylabel('Bottom Accelerometer(g)');
xlim([0 t_n]);          ylim([-10 10]);
grid on;                legend('Raw Data','Location','SouthWest');
set(gcf,'NextPlot','add');
axes; h = title(filename,'FontSize', 20);
set(gca,'Visible','off'); set(h,'Visible','on');

%Plot of flow meter data overlaid with response data
figure(3);              [AX,H1,H2]=plotyy(t,ch4,t,ch0);
tick1=[10 20 30 40 50 60];
axes(AX(1));            set(H1(1),'Color','b');
set(AX(1),'YColor','k','YTick',tick1);
xlabel('Time(s)');      ylabel('Flow (L/min)');
xlim([0 t_n]);          ylim(AX(1),[-1 40]);
tick2=[-10 0 10];       grid on;
axes(AX(2));            set(H2(1),'Color','r');
set(AX(2),'YColor','r','YTick',tick2);
ylabel('Bottom Accelerometer(g)');
xlim([0 t_n]);          ylim(AX(2),[-10 10]);
H2.Color(4)=.2;
set(gcf,'NextPlot','add');
axes; h = title(filename,'FontSize', 20);
set(gca,'Visible','off'); set(h,'Visible','on');

%Plot of input data.  Compare filtered to unfiltered.
figure(4);
plot(t,ch1,'r');        hold on;
plot(t,y1,'b');         grid on;
xlabel('Time(s)');      ylabel('Load Cell (g)');
xlim([0 t_n]);          ylim([-5 5]);
legend('Raw Data','Filtered','Location','SouthWest');
set(gcf,'NextPlot','add');
axes; h = title(filename,'FontSize', 20);
set(gca,'Visible','off'); set(h,'Visible','on');

%Plot of response data.  Compare filtered to unfiltered.
figure(5);
plot(t,ch0,'r');        hold on;
plot(t,y,'b');          grid on;
xlabel('Time(s)');      ylabel('Bottom Accelerometer (g)');
xlim([0 t_n]);          ylim([-10 10]);
```

```
legend('Raw Data','Filtered','Location','SouthWest')
set(gcf,'NextPlot','add');
axes; h = title(filename,'FontSize', 20);
set(gca,'Visible','off'); set(h,'Visible','on');

%Plot of input data equation - not needed for random data sets
figure(6);
plot(t,input,'b');      grid on;
xlabel('Time(s)');      ylabel('Input Frequency (Hz)');
xlim([0 t_n]);
set(gcf,'NextPlot','add');
axes; h = title(filename,'FontSize', 20);
set(gca,'Visible','off'); set(h,'Visible','on');

%%%%%%%%%%%%%%%%%%%%%%%%%%%%%%%%%%%%%%%%%%%%%%%%%%%%%%%%%%%%%%%%%%%%%%%%%%%%%%%
%And now for the FRF
%FRF of unfiltered data
response=fft(ch0);              force=fft(ch1);
response1=abs(response);        force1=abs(force);
Response=response1(1:L);        Force=force1(1:L);
FRF=Response./Force;            freq=linspace(0,N,L);

%filtered FRF data
responsef=fft(y);               forcef=fft(ch1);
response1f=abs(responsef);      force1f=abs(forcef);
Response1f=response1f(1:L);     Forcef=force1f(1:L);
FRFf1=Response1f./Forcef;

%Add a median filter to eliminate the narrow spikes in the data
FRFf2=medfilt1(FRFf1,100);
FRFf=smooth(FRFf2);

%Plot of unfiltered FRF
figure(7);                      loglog(freq,FRF,'r');
xlim([20 freqmax]); ylim([.01 100]);
xlabel('frequency'); ylabel('Acceleration filtered (g)');
title(filename,'FontSize', 20); grid on
legend('Original Signal','Filtered Data','Location','SouthWest')

%plot of unfiltered and filtered data superimposed
figure(8);                      loglog(freq,FRF,'r')
hold on;                        loglog(freq,FRFf,'b')
xlim([20 freqmax]); ylim([.01 100]);
xlabel('frequency'); ylabel('Acceleration filtered (g)');
title(filename,'FontSize', 20); grid on
legend('Original Signal','Filtered Data','Location','SouthWest')

%plot just the filtered FRF by itself
figure(9);                      loglog(freq,FRFf,'b')
xlim([20 freqmax]); ylim([.01 100]);
xlabel('frequency'); ylabel('Acceleration (g)');
title(filename,'FontSize', 20); grid on
```

```
%%%%%%%%%%%%%%%%%%%%%%%%%%%%%%%%%%%%%%%%%%%%%%%%%%%%%%%%%%%%%%%%%%%%%%%%%%%%
%determining which frequency at which each major mode occurs
fprintf(' \n')
fprintf(filename)
fprintf(' \n')

from1=ceil(t_n*minimum1);       to1=ceil(t_n*maximum1);
from2=ceil(t_n*minimum2);       to2=ceil(t_n*maximum2);
from3=ceil(t_n*minimum3);       to3=ceil(t_n*maximum3);

mode1 = FRFf(from1:to1);        freqmode1=freq(from1:to1);
%snip mode 1 from FRF
[Amax1,I1] = max(mode1);        mid1 = I1+from1;
%find Amax for mode 1
frmode1=freq(mid1);             %find fr for mode 1
halfbandmode1 = Amax1/sqrt(2);  %find halfband line
leftmode1=FRFf(from1:mid1);     rightmode1=FRFf(mid1:to1);
%separate left and right halves
[diffl1,idleft1] = min(abs(leftmode1-halfbandmode1));
%find where crosses left
[diffr1,idright1] = min(abs(rightmode1-halfbandmode1));
%find where crosses right
IDleft1 = idleft1+from1;        IDright1=idright1+mid1;
%convert to location on full spectrum
famode1 = freq(IDleft1);        fbmode1 = freq(IDright1);
%calc fa and fb for mode 1

mode2 = FRFf(from2:to2);        freqmode2=freq(from2:to2);
%snip mode 2 from FRF
[Amax2,I2] = max(mode2);        mid2 = I2+from2;
%find Amax for mode 2
frmode2=freq(mid2);             %find fr for mode 2
halfbandmode2 = Amax2/sqrt(2);  %find halfband line
leftmode2=FRFf(from2:mid2);     rightmode2=FRFf(mid2:to2);
%separate left and right halves
[diffl2,idleft2] = min(abs(leftmode2-halfbandmode2));
%find where crosses left
[diffr2,idright2] = min(abs(rightmode2-halfbandmode2));
%find where crosses right
IDleft2 = idleft2+from2;        IDright2=idright2+mid2;
%convert to location on full spectrum
famode2 = freq(IDleft2);        fbmode2 = freq(IDright2);
%calc fa and fb for mode 2

mode3 = FRFf(from3:to3);        freqmode3=freq(from3:to3);
%snip mode 3 from FRF
[Amax3,I3] = max(mode3);        mid3 = I3+from3;
%find Amax for mode 3
frmode3=freq(mid3);                 %find fr for mode 3
halfbandmode3 = Amax3/sqrt(2);      %find halfband line
leftmode3=FRFf(from3:mid3);     rightmode3=FRFf(mid3:to3);
%separate left and right halves
```

```
[diffl3,idleft3] = min(abs(leftmode3-halfbandmode3));
%find where crosses left
[diffr3,idright3] = min(abs(rightmode3-halfbandmode3));
%find where crosses right
IDleft3 = idleft3+from3;        IDright3=idright3+mid3;
%convert to location on full spectrum
famode3 = freq(IDleft3);        fbmode3 = freq(IDright3);
%calc fa and fb for mode 3

fprintf('-----Mode 1-----.\n');
fprintf('fr is %2.2f Hz.\n',frmode1);
fprintf('fa is %2.2f g.\n',famode1);
fprintf('fb is %2.2f g.\n',fbmode1);
fprintf('Amax is %2.2f g.\n',Amax1);

fprintf('-----Mode 2-----.\n');
fprintf('fr is %2.2f Hz.\n',frmode2);
fprintf('fa is %2.2f g.\n',famode2);
fprintf('fb is %2.2f g.\n',fbmode2);
fprintf('Amax is %2.2f g.\n',Amax2);

fprintf('-----Mode 3-----.\n');
fprintf('fr is %2.2f Hz.\n',frmode3);
fprintf('fa is %2.2f g.\n',famode3);
fprintf('fb is %2.2f g.\n',fbmode3);
fprintf('Amax is %2.2f g.\n',Amax3);

%plot each mode and see if we can get that halfband plotted on there
figure(10);                     subplot(131)
loglog(freqmode1,mode1,'b');    xlim([minimum1 maximum1]);
X1=[minimum1 maximum1];         Y1=[halfbandmode1 halfbandmode1];
hold on;                        loglog(X1,Y1);
xlabel('frequency (Hz)');       ylabel('acceleration (g)');
grid on;                        title({' ';' ';'Mode 1'});

subplot(132)
loglog(freqmode2,mode2,'b');    xlim([minimum2 maximum2]);
X2=[minimum2 maximum2];         Y2=[halfbandmode2 halfbandmode2];
hold on;                        loglog(X2,Y2);
xlabel('frequency (Hz)');       ylabel('acceleration (g)');
grid on;                        title({' ';' ';'Mode 2'});

subplot(133)
loglog(freqmode3,mode3,'b');    xlim([minimum3 maximum3]);
X3=[minimum3 maximum3];         Y3=[halfbandmode3 halfbandmode3];
hold on;                        loglog(X3,Y3);
xlabel('frequency (Hz)');       ylabel('acceleration (g)');
grid on;                        title({' ';' ';'Mode 3'});

%This just puts the title at the top of the subplots
set(gcf,'NextPlot','add');
axes; h = title({filename;' '},'FontSize', 20);
```

```
set(gca,'Visible','off'); set(h,'Visible','on');

%%%%%%%%%%%%%%%%%%%%%%%%%%%%%%%%%%%%%%%%%%%%%%%%%%%%%%%%%%%%%%%%%%%%%%%%%%%%
%Now let's calculate some Q-factor values
Qmode1=(frmode1/(fbmode1-famode1));
Qmode2=(frmode2/(fbmode2-famode2));
Qmode3=(frmode3/(fbmode3-famode3));

fprintf('-----Q-factors-----.\n');
fprintf('Q mode 1 is %2.2f.\n',Qmode1);
fprintf('Q mode 2 is %2.2f.\n',Qmode2);
fprintf('Q mode 3 is %2.2f.\n',Qmode3);

%%%%%%%%%%%%%%%%%%%%%%%%%%%%%%%%%%%%%%%%%%%%%%%%%%%%%%%%%%%%%%%%%%%%%%%%%%%%
%velocity and displacement
%Snip the major modes from response
mode1a = ch0(ceil(tmode11*Fs):ceil(tmode12*Fs));   %snip mode 1 from
response and time
mode2a = ch0(ceil(tmode21*Fs):ceil(tmode22*Fs));   %snip mode 2 from
response and time
mode3a = ch0(ceil(tmode31*Fs):ceil(tmode32*Fs));   %snip mode 3 from
response and time

%Snip the time domain to match
t1 = t(ceil(tmode11*Fs):ceil(tmode12*Fs));
t2 = t(ceil(tmode21*Fs):ceil(tmode22*Fs));
t3 = t(ceil(tmode31*Fs):ceil(tmode32*Fs));

%Find acceleration at the peak
tmax1=find(mode1a==max(mode1a));        a1=mode1a(tmax1);
tmax2=find(mode2a==max(mode2a));        a2=mode2a(tmax2);
tmax3=find(mode3a==max(mode3a));        a3=mode3a(tmax3);

%calculate the displacement in meters
Xon1=((g*a1)/(2*pi^2*frmode1^2))*1000;      %displacement in meters
Xon2=((g*a2)/(2*pi^2*frmode2^2))*1000;      %displacement in meters
Xon3=((g*a3)/(2*pi^2*frmode3^2))*1000;      %displacement in meters

fprintf('-----Displacement-----.\n');
fprintf('Xon mode 1 is %2.5f.\n',Xon1);
fprintf('Xon mode 2 is %2.5f.\n',Xon2);
fprintf('Xon mode 3 is %2.5f.\n',Xon3);

%%%%%%%%%%%%%%%%%%%%%%%%%%%%%%%%%%%%%%%%%%%%%%%%%%%%%%%%%%%%%%%%%%%%%%%%%%%%
%Once I have the Q factor for each system, I can sum up the energy of all
%the modes and get the total energy of that system.
omega1=frmode1*2*pi;
omega2=frmode2*2*pi;
omega3=frmode3*2*pi;

Wmode1=(mass*(Qmode1^-1)*(omega1^3)*(Xon1/1000^2))/2;%energy of first mode
Wmode2=(mass*(Qmode2^-1)*(omega2^3)*(Xon2/1000^2))/2;%energy of 2nd mode
```

```
Wmode3=(mass*(Qmode3^-1)*(omega3^3)*(Xon3/1000^2))/2;%energy of third mode

Wtot=Wmode1+Wmode2+Wmode3;                          %total energy of system

fprintf('-----Energy-----.\n');
fprintf('W mode 1 is %2.2f.\n',Wmode1);
fprintf('W mode 2 is %2.2f.\n',Wmode2);
fprintf('W mode 3 is %2.2f.\n',Wmode3);
fprintf('W total is %2.2f.\n',Wtot);

%%%%%%%%%%%%%%%%%%%%%%%%%%%%%%%%%%%%%%%%%%%%%%%%%%%%%%%%%%%%%%%%%%%%%%%%%%%%
%Now calculate the heat lost by the system.
%Only applicable to liquid nitrogen tests
energy=0;
for i=1:numpoints;
    energydt=(hVap*rho*(1/1000)*ch4(i)*dt)/60;
    energy=energy+energydt;
end
fprintf('-----Thermal Energy-----.\n');
fprintf('Total Thermal Energy lost is %2.0f.\n',energy);

%maximum flow rate at the peak
flowmax=max(ch4);
fprintf('-----Peak Flow-----.\n');
fprintf('Peak Flow is %2.2f.\n',flowmax);
```

LIST OF REFERENCES

[1] R. G. Scurlock, "The Future With Cryogenic Fluid Dynamics," *Physics Procedia,* vol. 67, pp. 20-26, 2015.

[2] R. Werlink, "Ten Liter Dewar Support Free Tank Shaker Vibration and Drop Shock Test Results," KSC NASA, Cape Canaveral, 2012.

[3] P. Lebrun, "An Introduction to Cryogenics," CERN, Accelerator Technology Deptartment, Switzerland, 2007.

[4] T. A. Tombrello, "Oscillating Systems," *Salem Press Encyclopedia of Science,* p. xxx, January 2015.

[5] J. D. Smith, Vibration Measurement and Analysis, London: Butterworths, 1989.

[6] M. P. Norton and D. G. Karczub, Fundamentals of Noise and Vibration Analysis for Engineers, Second Edition ed., Cambridge: Cambridge University Press, 2003.

[7] M. Kutz, Handbook of Measurement in Science and Engineering, vol. 1, Hoboken: John Wiley & Sons, Inc, 2013.

[8] J. H. Harlow, Electric Power Transformer Engineering, Boca Raton, FL: CRC Press LLC, 2004.

[9] B. A. Olmos and J. M. Roesset, "Evaluation of the Half-Power Bandwidth Method to Estimate Damping in Systems Without Real Modes," *Earthquake Engineering and Structural Dynamics,* pp. 1671-1686, 2010.

[10] S. Butterworth, "On the Theory of Filter Amplifiers," *Experimental Wireless and the Wireless Engineer,* vol. 7, pp. 536-541, 1930.

[11] M. Arriagada and M. Partl, "Calculation of Displacements of Measured Accelerations, Analysis of Two Accelerometers and Application in Road Engineering," in *6th Swiss Transport Research Conference*, Monte Verita, 2006.

[12] W. T. Thomson and M. D. Dahleh, Theory of Vibration with Applications, Bejing: Tsinghua University, 2005.

[13] T. Woods, "Aerogels: Thinner, Lighter, Stronger," NASA's Glenn Research Center, 28 July 2011. [Online]. Available: http://www.nasa.gov/topics/technology/features/aerogels.html. [Accessed 22 February 2016].

[14] Cabot Corporation, "Cabot Aerogel Particles Datasheet," Cabot Corporation Business and Technical Center, Billerica, MA, 2013.

[15] Unholtz-Dickie Corporation, "Electrodynamic Shaker Systems," Unholtz-Dickie Corporation, [Online]. Available: http://www.udco.com/hseries.shtml. [Accessed 22 Feb 2016].

[16] E. Sauther, "Sine Sweep Vibration Testing for Modal Response Primer," Department of Optical Sciences, University of Arizona, Tuscon, 2013.